Energy and Electron Transfer in Polyacetylene-Linked Zinc–Porphyrin–[60]Fullerene Molecular Wires

Sean A. Vail,[a] Paul J. Krawczuk,[a] Dirk M. Guldi,[b] Amit Palkar,[c] Luis Echegoyen,[c] Joao P. C. Tomé,[a] Michael A. Fazio,[a] and David I. Schuster*[a]

Abstract: The synthesis and electrochemical and photophysical studies of a series of alkyne-linked zinc–porphyrin–[60]fullerene dyads are described. These dyads represent a new class of fully conjugated donor–acceptor systems. An alkynyl–fullerene synthon was synthesized by a nucleophilic addition reaction, and was then oxidatively coupled with a series of alkynyl tetraaryl zinc–porphyrins with 1–3 alkyne units. Cyclic and differential pulse voltammetry studies confirmed that the porphyrin and fullerene are electronically coupled and that the degree of electronic interaction decreases with increasing length of the alkyne bridge. In toluene, energy transfer from the excited zinc–porphyrin singlet to the fullerene moiety occurs, affording fullerene triplet quantum yields of greater than 90%. These dyads exhibit very rapid photoinduced electron transfer in tetrahydrofuran (THF) and benzonitrile (PhCN), which is consistent with normal Marcus behavior. Slower rates for charge recombination in THF versus PhCN clearly indicate that charge-recombination events are occurring in the Marcus inverted region. Exceptionally small attenuation factors (β) of 0.06 ± 0.005 Å^{-1} demonstrate that the triple bond is an effective mediator of electronic interaction in zinc–porphyrin–alkyne–fullerene molecular wires.

Keywords: alkynes · conjugation · electron transfer · fullerenes · porphyrinoids

Introduction

The rational design of novel, artificial, photosynthetic ensembles has emerged as a topic of major interest in the fields of chemistry and biology.[1] One of the most remarkable properties of [60]fullerene (C_{60}) as an acceptor in electron-transfer (ET) processes is that it gives rise to an efficient and rapid photoinduced charge separation (CS) and slow charge recombination (CR) in the dark.[2] Porphyrin–[60]fullerene dyads exhibit long-lived charge-separated states, which in a few cases have been successfully used to generate photocurrents.[3] Although various spacers have been utilized in attempts to enhance the interaction between donors and acceptors, the use of "molecular wires" as bridging components in donor–acceptor systems has been proven to be one of the most promising approaches for establishing efficient communication between the chromophores.[4]

Incorporation of molecular wires into conjugated donor–acceptor (D–A) systems has emerged as a promising strategy for constructing molecular electronic materials.[5] Such molecules have already found applications in electrical conductors,[6] photovoltaic cells,[7] electroluminescent devices,[8] nonlinear optics,[9] and field-effect transistors.[10] Efficient long-range ET and energy-transfer (EnT) phenomena have

[a] S. A. Vail, P. J. Krawczuk, J. P. C. Tomé, M. A. Fazio, Prof. Dr. D. I. Schuster
Department of Chemistry, New York University
100 Washington Square East, New York, NY 10003 (USA)
Fax: (+1) 212-260-7905
E-mail: david.schuster@nyu.edu

[b] Prof. Dr. D. M. Guldi
University of Erlangen
Institute for Physical and Theoretical Chemistry
91058 Erlangen (Germany)

[c] A. Palkar, Prof. Dr. L. Echegoyen
Department of Chemistry, Clemson University
519 Hunter Laboratories, Clemson, SC 29634 (USA)

Supporting information for this article is available on the WWW under http://www.chemeurj.org/ or from the author. It contains UV/Vis absorption spectra of compounds **3**, **5**, and **7** (Figure S1), **4** and **9** (Figure S2), **8** and **11** (Figure S3); cyclic voltammograms and differential pulse voltammograms of compounds **5**, **6**, and **9** (Figures S4 and S5), **7**, **8**, and **10** (Figures S6 and S7) and dyad **11** (Figures S8 and S9); a variable scan plot for compound **4** (Figure S10); molecular modeling calculations for compounds **9**, **10**, and **11** (Figure S11); MALDI-TOF mass spectra for compounds **1**–**11** (Figures S12–S22); 200 MHz ^{1}H NMR spectra of compounds **1** and **2** (Figures S23 and S24); 400 MHz ^{1}H NMR spectra of compounds **3**–**11** (Figures S25–S33).

 DOI: 10.1002/chem.200401348

been observed in systems possessing redox centers connected by molecular wires.[4,11–19] As it is known that the efficiency of ET decreases exponentially with increasing molecular-wire length, and that the attenuation factor is a function of the electronic structure and overall architecture of the wire,[11–20] much effort has been devoted to designing systems that facilitate long-range ET and EnT processes.[21] The attenuation factor (β), which describes the intrinsic electronic properties of the bridge, is related to the distance dependence of electron-transfer rate constants (k_{ET}) as shown in Equation (1):

$$k_{ET} = k_0 \exp(-\beta R_{DA}) \quad (1)$$

in which k_0 is a kinetic prefactor and R_{DA} is the D–A center-to-center distance.[22] Recently, it has been shown that effective matching of orbital energies between the donor and bridge components is a necessary consideration for achieving efficient "molecular-wire" behavior in conjugated D–A systems.[22,23]

Oligothiophenes have been shown to be good candidates for studying the efficiency of molecular-wire behavior due to their ready accessibility, ease of structural modification, high π conjugation, and low oxidation potentials.[24,25] Ito and co-workers have used extended oligothiophene chains as rigid covalent linkers between versatile electro- and photoactive compounds, including porphyrins and fullerenes.[12] In a photoactive triad system consisting of a porphyrin–oligothiophene–[60]fullerene assembly, an attenuation factor (β) of 0.11 $Å^{-1}$ was determined from a plot of $\ln k_{ET}$ versus R_{DA}. This value is significantly smaller than those obtained for saturated hydrocarbon bridges[13] ($\beta = 0.6$–1.2 $Å^{-1}$) and conjugated paraphenylenes[14] ($\beta = 0.32$–0.66 $Å^{-1}$), but is comparable to oligoenes[15,16] ($\beta = 0.04$–0.2 $Å^{-1}$) and oligoynes[16b,17] ($\beta = 0.04$–0.17 $Å^{-1}$).

More recently, Martín and co-workers reported an exceptionally small attenuation factor ($\beta = 0.01 \pm 0.005$ $Å^{-1}$) for a series of exTTF–wire–C_{60} ensembles made by incorporating oligo(phenylenevinylene)s (oligo(PPV)s) as bridges between π-extended tetrathiafulvalene (exTTF) donors and [60]fullerene acceptor moieties.[18] Homoconjugation is achieved by coupling of the exTTF moiety to the fullerene sphere through the oligomeric bridge. This series of exTTF–wire–C_{60} systems exhibits excellent molecular-wire behavior over distances of up to 40 Å. Donor–acceptor coupling constants (V) of ~5.5 cm^{-1} reflect strong electronic coupling through the paraconjugation of the oligo(PPV)s to the exTTF donor, which promotes charge-transfer phenomena with a weak dependence on molecular distance.

Recent studies of long-range charge separation (CS) in D–A systems have shown that π-conjugated polyene and polyyne spacers dramatically enhance electronic coupling between donors and acceptors.[26] Although free rotation about single bonds can lead to variations in donor–acceptor distances as well as reduced conjugation in polyene-linked D–A systems,[27] polyyne linkers maintain fixed distances between the chromophores and permit enhanced conjugation in rigid D–A systems, affording geometrically well-defined materials that simplify the interpretation of physical data. Schuster et al. and Yamada et al. were among the first to report on the study of porphyrin–C_{60} (D–A) systems linked by an alkyne bridge.[28] Although no *true* conjugation was present in Yamada's fulleropyrrolidine derivative, which has an intervening sp^3 carbon atom, the accelerated rate of CS over an analogous amide-linked system can be rationalized in terms of enhanced electronic coupling between the porphyrin and fullerene moieties.[28b]

Komatsu and co-workers were the first to report the synthesis and study of trimethylsilylethynyl– and phenylethynyl–hydrofullerenes, the first alkyne–C_{60} derivatives,[29] prepared by nucleophilic addition of the appropriate alkynyllithium reagent to the fullerene, followed by quenching with trifluoroacetic acid. Diederich and co-workers studied the chemistry of a variety of fullerene–acetylene hybrids,[30] leading to significant progress in the synthesis of carbon allotropes incorporating fullerenes around a central acetylenic framework.

We recently reported the synthesis and preliminary photophysical study of the first completely conjugated butadiyne-linked zinc–porphyrin–[60]fullerene (ZnP–C_{60}) dyad,[19] in which the two chromophores were linked by a *fully* conjugated "molecular wire" with no intervening sp^3 carbons. Upon photoexcitation, this system exhibited both extremely rapid forward ET and slower charge-recombination (CR) dynamics. Steady-state fluorescence studies in chloroform revealed that the porphyrin fluorescence was almost entirely quenched by the attached fullerene moiety, while the fluorescence lifetime (τ_f) of less than 10 ps indicated rapid and efficient communication between the chromophores.

We now report a complete photophysical and electrochemical investigation of a series of rigid polyalkynyl-linked zinc–porphyrin–[60]fullerene dyads in which CS and CR processes were studied as a function of D–A distance.

Results and Discussion

Synthesis: The synthesis of 1-ethynyl-2-methyl[60]fullerene (**2**) was carried out according to the methodology previously reported for the corresponding benzyl derivative.[31] As shown in Scheme 1, nucleophilic addition of lithium trimethylsilylacetylide to C_{60}, followed by quenching with excess iodomethane, furnished **1** in ~50% yield. Deprotection of

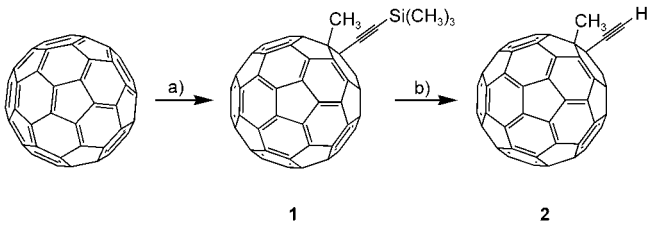

Scheme 1. Synthesis of 1-ethynyl-2-methyl[60]fullerene (**2**): a) 1. Li–≡–$SiMe_3$, 2. CH_3I/THF/40 °C; b) K_2CO_3, THF/CH_3OH/△.

the alkyne with potassium carbonate in refluxing THF/CH_3OH (5:1) afforded fullerene derivative **2** in ~45% yield.

Zinc(II)–5-[4-(trimethylsilylethynyl)phenyl]-10,15,20-*tris*[3,5-di(*tert*-butyl)phenyl]porphyrin (**3**) was synthesized by modification of the one-step nitrobenzene method previously reported (Scheme 2).[32] Condensation of the mixed aldehydes with pyrrole in a refluxing solution of glacial acetic acid/nitrobenzene (4:3) furnished a crude mixture of porphyrins, which was metalated by treatment with zinc acetate dihydrate in refluxing chloroform/methanol (2:1) for four hours. Zinc–porphyrin **3** was effectively isolated using a long silica-gel column with cyclohexane/methylene chloride (4:1) as the eluent. Zinc–porphyrin **3** was deprotected with excess tetrabutylammonium fluoride hydrate (TBAF) in tetrahydrofuran at room temperature, affording **4** as a purple, crystalline solid in near quantitative yield.

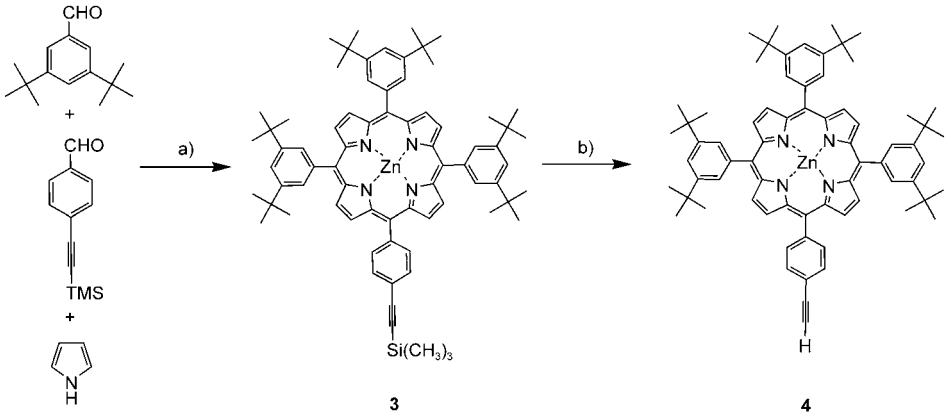

Scheme 2. Synthesis of zinc(II)–5-(4-ethynylphenyl)-10,15,20-tris[3,5-di(*tert*-butyl)phenyl]porphine (**4**): a) 1. acetic acid, nitrobenzene, △, 2. $Zn(OAc)_2$; b) TBAF.

Extended TMS-protected (TMS = trimethylsilyl) alkynyl zinc–porphyrins **5** and **7** were prepared by oxidative heterocoupling with excess trimethylsilylacetylene under a dry oxygen atmosphere (Scheme 3). The oxidative heterocoupling reaction, utilizing in situ preparation of the Hay catalyst (CuCl–TMEDA–O_2; TMEDA = *N*,*N*,*N*′,*N*′-tetramethylethylenediamine) in freshly distilled methylene chloride, furnished **5** and **7** in quantitative yield. These compounds were then treated with an excess of TBAF hydrate at room temperature to furnish the respective deprotected alkynyl zinc–porphyrins **6** and **8** in quantitative yield.

Polyalkynyl–ZnP–C_{60} dyads **9**, **10**, and **11** were synthesized by oxidative heterocoupling reactions between ethynyl fullerene derivative **2** and an excess of zinc–porphyrins **4**, **6**, and **8** (Scheme 4). Oxidative coupling, again with in situ preparation of the Hay catalyst in chlorobenzene under a dry oxygen atmosphere, afforded nonfluorescent dyads **9**, **10**, and **11** in modest yields, along with products identified by MALDI-TOF mass spectra as alkynyl-linked homodimers ZnP–ZnP and C_{60}–C_{60} formed under the reaction conditions. Each ZnP–C_{60} dyad was separated from its corresponding homocoupling products on a silica funnel using CS_2 as the eluent. The ZnP–C_{60} dyads eluted before

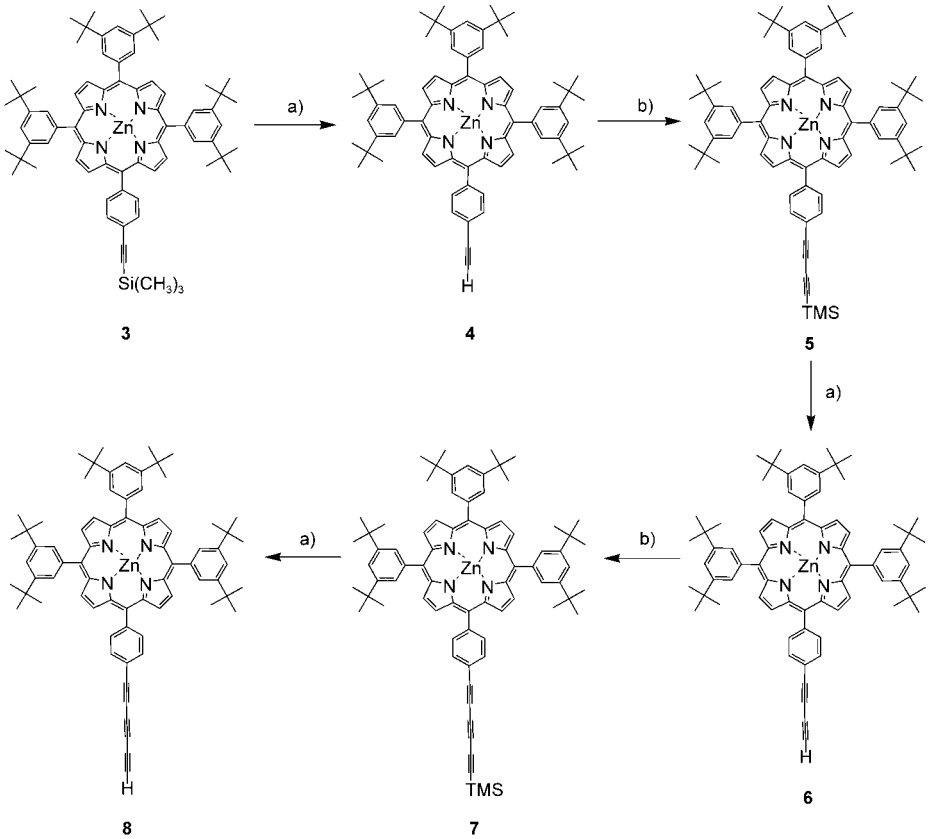

Scheme 3. Synthesis of zinc(II)–5-(4-alkynylphenyl)-10,15,20-tris[3,5-di(*tert*-butyl)phenyl]porphyrins **4**, **5**, **6**, **7**, and **8**: a) TBAF; b) TMS–≡–H, CuCl/TMEDA.

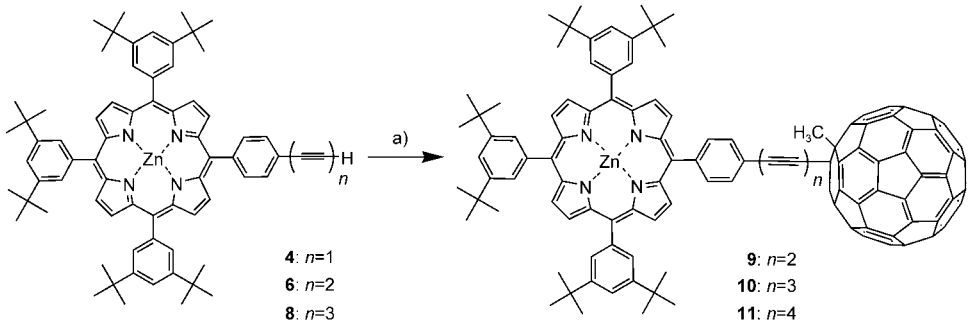

Scheme 4. Synthesis of zinc(II)–5-(4-alkynylphenyl)-10,15,20-tris[3,5-di(*tert*-butyl)phenyl]porphyrin-1-ethynyl-2-methyl[60]fullerene dyads **9**, **10**, and **11**: a) **2**, chlorobenzene/CuCl, TMEDA.

the ZnP–ZnP dimers, whereas the C_{60}–C_{60} dimer was retained on the silica. ZnP–C_{60} dyads **9**, **10**, and **11** were further purified by preparative thin-layer chromatography (TLC) on silica gel using CS_2 as the eluent. The purity of all samples was confirmed by TLC, ^{1}H NMR, and MALDI-TOF analysis.

Structural characterization: Compounds **1**–**11** were fully characterized by UV/Vis, ^{1}H NMR, and MALDI-TOF mass spectrometry. Full details and assignments are given in the Experimental Section.

Electronic absorption spectra: The UV/Vis absorption spectra for TMS-protected, polyalkynyl ZnP derivatives **3**, **5**, and **7** are depicted in Figure S1 in the Supporting Information. The spectra for all three porphyrins are virtually superimposable, exhibiting λ_{max} at 423, 425, and 425 nm, respectively. The UV/Vis absorption spectra for the deprotected ZnP analogues, **4**, **6**, and **8**, depicted in Figure 1, are also virtually superimposable, exhibiting λ_{max} at 423, 424, and 424 nm, respectively. Thus, extending the linker attached to ZnP has virtually no effect on the UV/Vis absorption spectra of these compounds. The spectra for ZnP–C_{60} dyads **9**, **10**, and **11**, depicted in Figure 2 and Figures S2 and S3 in the Supporting Information, all show strong absorption bands for both the porphyrin and fullerene moieties, and are consistent with the UV-visible spectra of other porphyrin–C_{60} systems.[33] Although a small red-shift in the spectra for dyads **9**, **10**, and **11** relative to zinc–porphyrins **4**, **6**, and **8** occurs, enhanced absorption by the dyads is not observed.

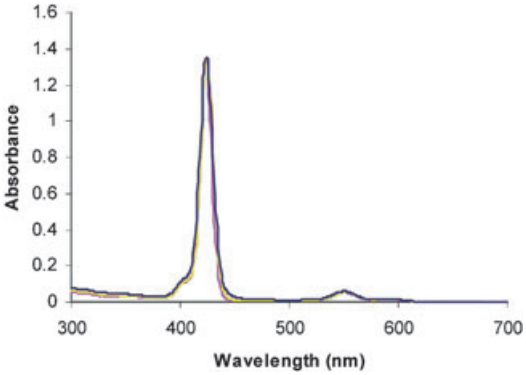

Figure 1. UV/Vis spectra of ZnP–alkynes **4** (pink), **6** (yellow), and **8** (blue) in chloroform (10 μM).

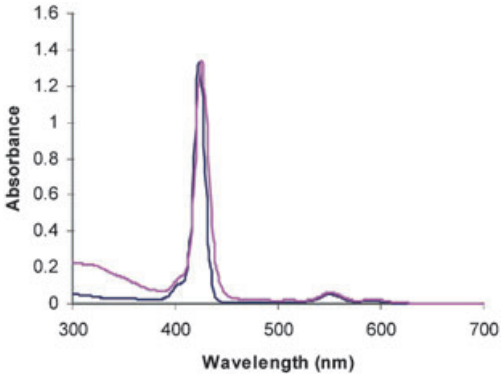

Figure 2. UV/Vis spectra of ZnP–alkyne **6** (blue) and ZnP–C_{60} dyad **10** (pink) in chloroform (10 μM).

Electrochemistry: As seen from the cyclic voltammogram (CV) illustrated in Figure 3, three reversible reduction waves are evident for alkynylfullerene **2** (see data summary in Figure 4). The reduction potentials are shifted cathodically relative to that of pristine C_{60},[27a] which is attributed to the saturation of one of the π bonds on the C_{60} surface.[29]

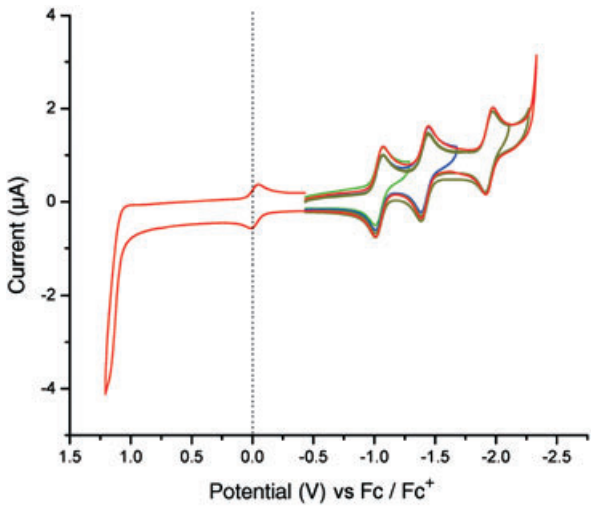

Figure 3. Cyclic voltammogram (CV) of **2**.

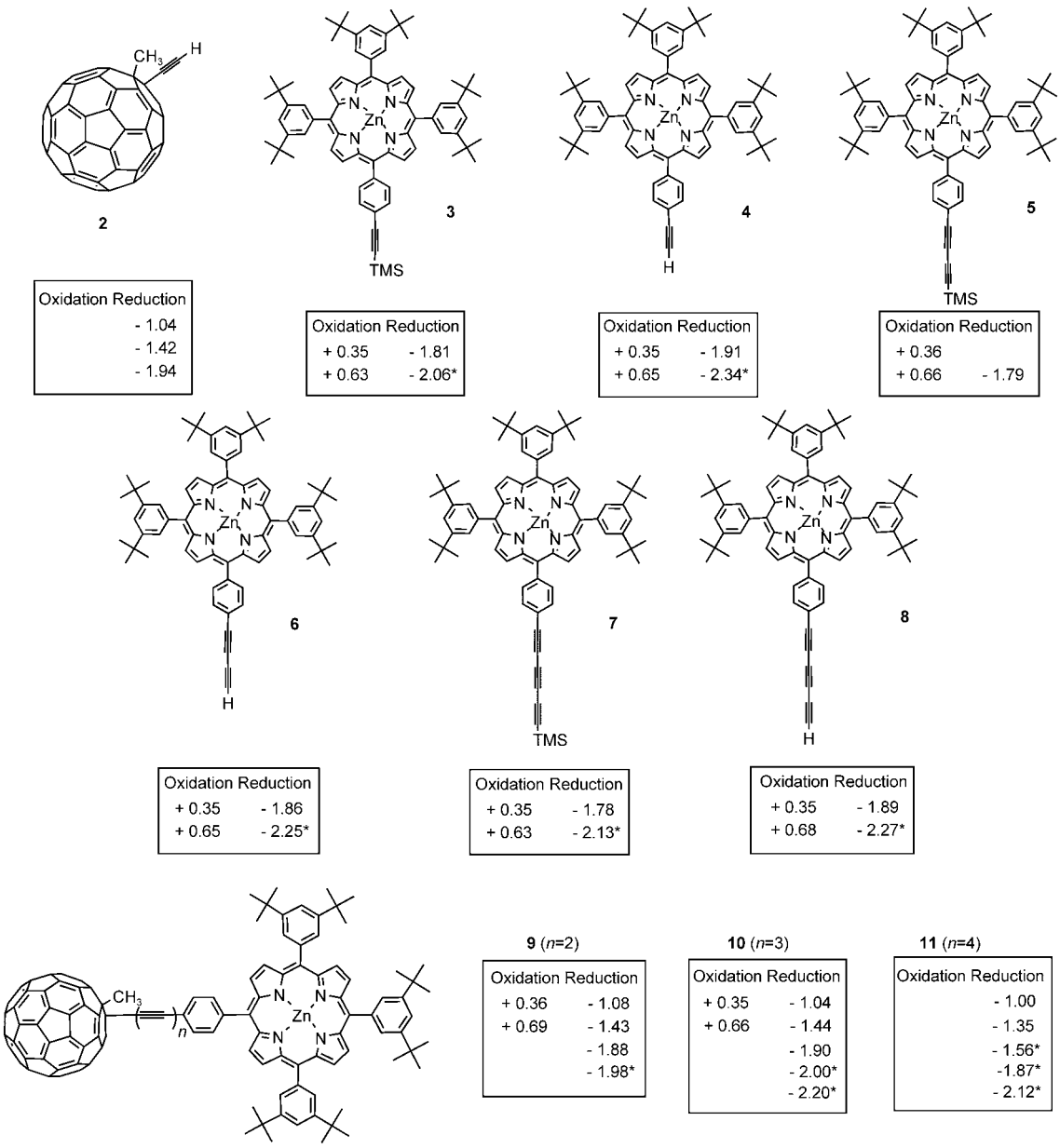

Figure 4. Oxidation and reduction potentials (V) of **1**–**11** versus Fc/Fc$^+$. The * indicates chemically irreversible peaks; therefore E_{max} is reported.

Differential pulse voltammetry (DPV) experiments show that the first oxidation of **2** occurs at $+1.18$ V. The peak potentials obtained from DPV experiments (Figure 5), were converted to $E_{1/2}$ values using Equation (2)[34]:

$$E_{max(DPV)} = E_{1/2} - \frac{\Delta E}{2} \quad (2)$$

in which ΔE is the pulse amplitude, and the values were found to be comparable to the potentials obtained from CV studies (Table 1).[35]

Figures 6 and 7 show the CV and DPV results of the zinc–porphyrins **3** and **4** with single acetylene groups, with TMS and H termini, respectively. Both compounds show two reduction and two oxidation peaks. Both oxidation peaks appear to be reversible and, from comparison with analogous compounds reported earlier,[27] are characteristic of porphyrin–acetylene systems. From the CV measurements, it can be seen that the reduction potential of **3** is about 100 mV more positive than that for **4**, reflecting the electropositive character of the trimethylsilyl group. The DPV results of these compounds show a similar trend to that observed in the CV experiments.

Figures S4 and S5 (Supporting Information) show the CV and DPV data of ZnP compounds **5** and **6** with diyne spacers. The compounds without the fullerene both show two oxidation and two reduction waves, similar to **3** and **4**. The positive shift of around 100 mV in the reduction poten-

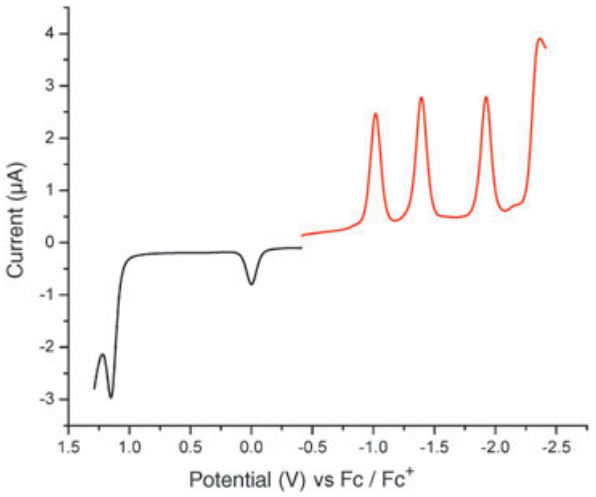

Figure 5. Differential pulse voltammogram (DPV) of **2**.

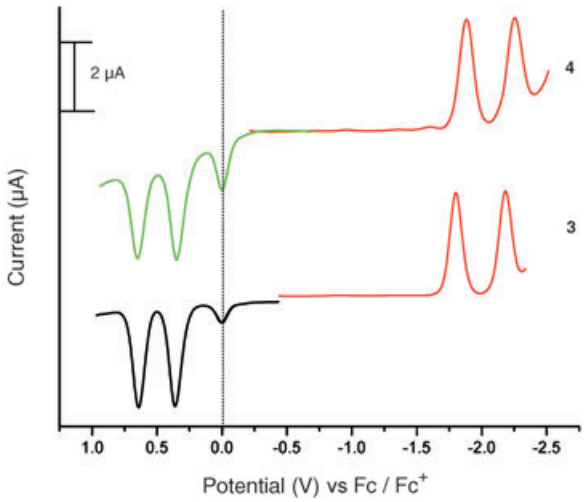

Figure 7. Differential pulse voltammogram (DPV) of **3** and **4**.

Table 1. Potentials (V) obtained from the DPV data versus Fc/Fc^+.[a]

Compounds	Reduction				Oxidation	
	E^1	E^2	E^3	E^4	E^1	E^2
2	−1.04	−1.42	−1.94			
3			−1.82	−2.19	0.37	0.67
4			−1.89	−2.21	0.38	0.68
5			−1.74	−2.08	0.38	0.67
6			−1.86	−2.16	0.35	0.66
7			−1.77	−2.11	0.38	0.70
8			−1.85	−2.16	0.37	0.67
9	−1.05	−1.43	−1.85	−2.08	0.36	0.68
10	−1.05	−1.40	−1.93	−2.12	0.38	0.72
11	−1.00	−1.34/−1.48	−1.82	−2.01	0.36	0.68

[a] Corrected using Equation (2).

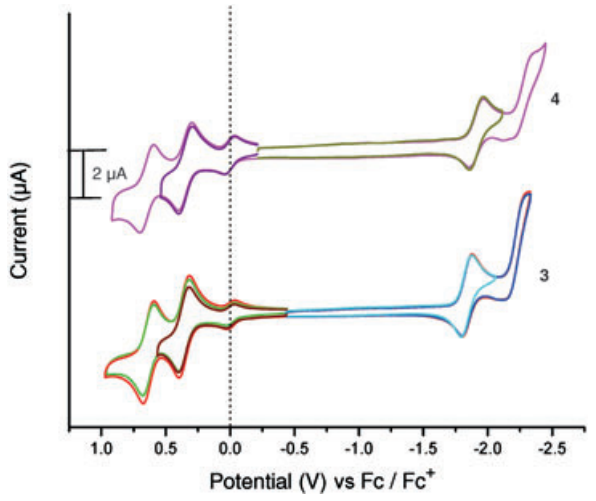

Figure 6. Cyclic voltammogram (CV) of **3** and **4**.

tial for **5** relative to **6** is again ascribed to the TMS group. The cathodic region of dyad **9** is dominated by reduction peaks characteristic of 1,2-disubstituted fullerenes.[28b] As observed for **2**, the first reduction peak shifts cathodically when pristine C_{60} is ethynylated. The first reduction potential of phenylethynyl–C_{60} is close to that of pristine C_{60} due to an anodic shift resulting from the electron-withdrawing inductive effect of the phenylethynyl group, which cancels out the cathodic shift that results from saturation of one of the π bonds on the surface of C_{60}.[29] Considering the structure of dyad **9**, in which a fullerene is connected to a phenyl group of tetraphenylporphine (TPP) by a butadiyne linkage, one would expect an effect similar to that seen for phenylethynyl–C_{60}. Counter intuitively, the first reduction potential of dyad **9**, which is fullerene-centered, shows a cathodic shift that is even larger than that observed for **2**, which can be explained if the porphyrin is electronically coupled with the fullerene in a donor–acceptor (D–A) interaction. A similar cathodic shift was seen in the DPV-derived potentials. We can not exclude the possibility that conjugation may also play a role in causing these cathodic shifts.

Comparison of the HOMO–LUMO gap of the dyads with those of their respective constituents supports this interpretation. The difference between the first oxidation and the first reduction potential, $E^{ox1}_{1/2} - E^{red1}_{1/2}$, as determined by CV, is a measure of the HOMO–LUMO gap. The HOMO–LUMO gap of the two components of dyad **9**, that is, zinc–porphyrin **6** and C_{60}, is ~1.33 V, while the HOMO–LUMO gap in dyad **9** is ~1.44 V, which is 110 mV larger.

The CV results for triacetylene compounds **7**, **8**, and **10**, with TMS, H, and C_{60} terminal groups, respectively, are shown in Figure S6 (Supporting Information). A similar trend to that observed in the previous series of compounds is apparent. As expected, zinc–trialkynylporphyrin **7**, with a TMS terminal, has a reduction potential 100 mV more positive than the corresponding compound **8** with an H terminus. The HOMO–LUMO gap in **10** determined from the CV potentials is ~1.39 V; this is larger than that of the individual fragments but lower than that found for dyad **9**, suggesting a decrease in electronic coupling, in accord with the larger porphyrin–C_{60} separation.

Compound **11**, with four acetylene spacers, shows four reduction peaks, two of which are reversible, and two reversible oxidation peaks (see Figure S8, Supporting Information). A comparison of the voltammetric response as a function of the distance between the redox-active moieties was then made for dyads **9**, **10**, and **11** (Figures 8 and 9). Compounds

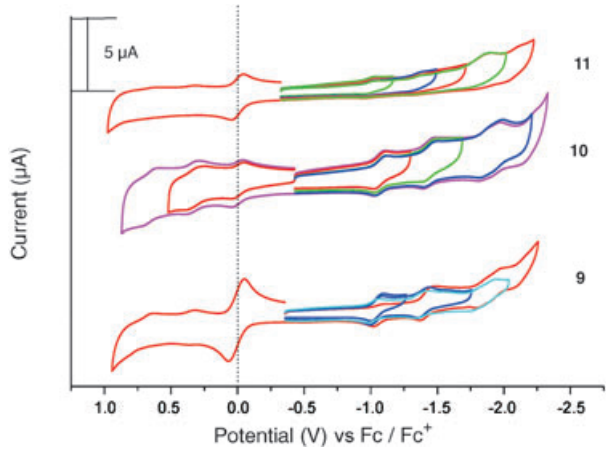

Figure 8. Cyclic voltammogram (CV) of **9**, **10**, and **11**.

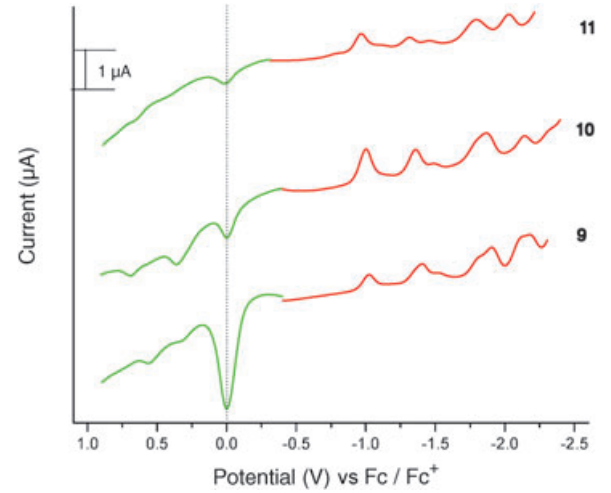

Figure 9. Differential pulse voltammogram (DPV) of **9**, **10**, and **11**.

9, **10**, and **11** have their first reduction potentials at −1.08 V, −1.04, and −1.00 V, respectively, showing electronic coupling between the donor–acceptor pair falls off with distance, which is attributed to a decrease in electron density on the fullerene. DPV data for dyad **11** showing the same trend is depicted in Figure S9 (Supporting Information). The splitting in the 3rd and 4th reduction potentials of **9**, ~−1.8 to −1.9 V and ~−2.1 to −2.2 V, respectively, is attributed to close overlap of the reduction waves of the porphyrin and fullerene moieties. The absence of such splitting in the 4th reduction peak in the DPV data for dyad **10** indicates decreased electronic coupling between the porphyrin and the fullerene. This interpretation is confirmed by the behavior of **11**, for which splitting in both the 3rd and 4th reduction peaks completely disappears. The shoulders observed around −1.5 V in the square wave voltammograms (Figure 9) are not currently understood. These are definitely not ascribable to dissolved oxygen. While we can not exclude the presence of trace impurities, the fact that these shoulders are seen for all three dyads makes this explanation less likely.

In order to determine the reversibility of the CV peaks, variable scan plots were recorded for all compounds. Sufficiently fast scan rates result in increased peak-to-peak separations. The variable scan plots for zinc–alkynylphenylporphyrin (**4**; Figure S10, Supporting Information) shows that peak-to-peak separations increase with increasing scan rates, indicating that these processes are quasi-reversible. Thus the $E_{1/2}$ values obtained from the CV data (Figure 3) are approximate, and vary slightly from those obtained from DPV experiments (Table 1). Similar results were obtained for all the other compounds except 1-ethynyl-2-methyl[60]fullerene (**2**), which shows completely reversible behavior upon reduction.

Photophysical studies: Zinc–tetraphenylporphine (ZnTPP) was used as the reference for comparison with the ZnP–(acetylene)$_n$–C$_{60}$ hybrids in steady-state fluorescence experiments, using normalized absorbance of 0.5 at the excitation wavelength (425 nm). In toluene, THF, and PhCN, the fluorescence quantum yield of ZnTPP is ~0.04.[36] Strong quenching occurs in ZnP–(acetylene)$_n$–C$_{60}$ systems with quantum yields of 1.6×10^{-3} for **11**, 0.9×10^{-3} for **10**, and 0.6×10^{-3} for **9**, all in toluene. Figure 10 shows the steady-state fluorescence of ZnP–(acetylene)$_n$–C$_{60}$ dyads and

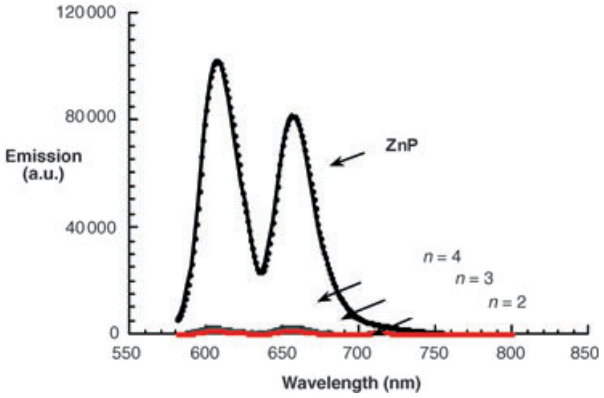

Figure 10. Room-temperature fluorescence spectra of ZnTPP and ZnP–(acetylene)$_n$–C$_{60}$ in toluene with absorbance of 0.5 at the 425 nm excitation wavelength. The red line indicates $n=2$.

ZnTPP in toluene. Quenching of ZnP fluorescence in the dyads shows a weak distance dependence. Although the yield drops, the emission patterns are not affected by the presence of the attached fullerene moiety. In addition to the ZnP transitions at 605 and 660 nm, a new emission band develops at 715 nm (see Figure 11), which does not correspond

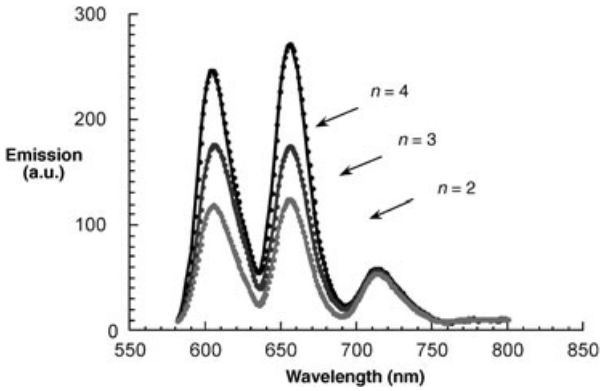

Figure 11. Room-temperature fluorescence spectra of ZnTPP and ZnP–(acetylene)$_n$–C$_{60}$ in toluene with absorbance of 0.5 at the 425 nm excitation wavelength.

to a ZnP-centered process, but is a reasonable match to C_{60} fluorescence.[2b] The observation of C_{60} fluorescence signifies a rapid intramolecular transduction of singlet excitation. The quantum yields for C_{60} fluorescence, measured in toluene, are constant at 0.3×10^{-3} for dyads **9**, **10**, and **11**.

The ZnP fluorescence yields for **11** in THF and PhCN are 1.1×10^{-3} and 0.9×10^{-3}, respectively, indicating increasingly faster deactivation of zinc–porphyrin singlet excited states (^{1}ZnP*) with increased solvent polarity, consistent with intramolecular electron transfer. The C_{60}-centered fluorescence is not seen in THF and PhCN, indicating that ET is taking place, rather than the EnT deactivation pathway seen in toluene.

From the fluorescence quantum yields (Φ_f) and lifetimes (τ) of photoexcited **9**, **10**, **11**, and ZnTPP (**X**),[37] the rate constant (k) for intramolecular EnT (in toluene) and ET (in THF and PhCN), in the ZnP–(acetylene)$_n$–C$_{60}$ dyads (**Y**), can be calculated according to Equation (3):

$$k(\mathbf{Y}) = [\Phi(\mathbf{X}) - \Phi(\mathbf{9}, \mathbf{10}, \mathbf{11})]/[\tau(\mathbf{X})\Phi(\mathbf{9}, \mathbf{10}, \mathbf{11})] \quad (3)$$

The rate constants, which range between 8×10^9 and 3.3×10^{10} s^{-1} in PhCN, are listed in Table 2.

The fate of ^{1}ZnP* and the identity of the photoproducts in the ZnP–(acetylene)$_n$–C$_{60}$ systems were examined by pico-, nano-, and microsecond transient absorption spectroscopy. Representative picosecond time-resolved absorption spectra for ZnTPP, taken after an 18 ps laser pulse at 532 nm in toluene solution, are displayed in Figure 12. The differential spectrum recorded immediately after the laser

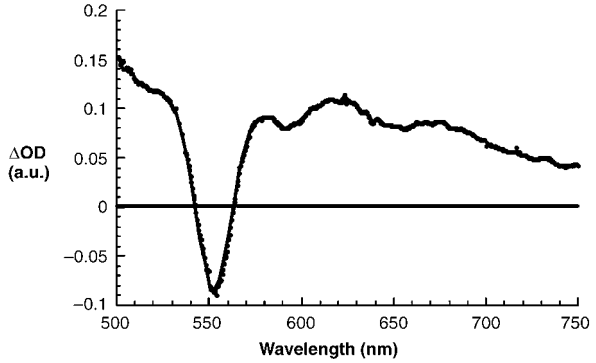

Figure 12. Differential absorption spectrum (visible and near-infrared) obtained upon picosecond flash photolysis (532 nm) of ~1.0×10^{-5} M solutions of the ZnTPP reference in nitrogen-saturated toluene with a time delay of 50 ps at room temperature. The spectrum corresponds to the singlet–singlet spectrum of ^{1}ZnTPP*.

pulse (50 ps time delay) is characterized by bleaching of the porphyrin Q-band absorption at 550 nm and the appearance of broad absorption between 570 and 750 nm. These are spectral attributes of ^{1}ZnP* (2.04 eV),[38] which decays slowly (4.0×10^8 s^{-1}) in toluene to the energetically lower-lying triplet excited state ^{3}ZnP* (1.53 eV) through intersystem crossing (ISC).[39] The formation of a pentacoordinated Zn complex in coordinating solvents, such as THF and PhCN, shifts the Q band slightly to the red region (565 nm), with respect to the noncoordinating solvent toluene.

In time-resolved transient absorption measurements in toluene for compounds **9**, **10**, and **11**, instantaneous growth of broad absorption between 570 and 750 nm confirms selective excitation of the ZnP moiety in the dyads. However, instead of observing the slow ISC dynamics (4.0×10^8 s^{-1}) exhibited by ZnTPP, the ^{1}ZnP* decay in the dyads is accelerated (~1×10^{10} s^{-1}) due to the presence of C_{60}. Spectroscopically, the changes in transient absorption, measured after completion of the decay, bear no resemblance to that of ZnP triplet excited states. The new transients reveal strong maxima at 880 nm, characteristic of C_{60} singlet excited states (^{1}C$_{60}$*).[38] In a fullerene reference, ISC ($k=5.0\times10^8$ s^{-1}) to the energetically lower-lying triplet state, ^{3}C$_{60}$*, dominates the deactivation of ^{1}C$_{60}$*.[40] The 880 nm transition decays with similar kinetics in the ZnP–(acetylene)$_n$–C$_{60}$ dyads in toluene. The only component seen in the complementary nanosecond experiments was due to decay of ^{3}C$_{60}$* ($\lambda_{max}=360$,

Table 2. Fluorescence quantum yields (Φ_f), rate constants for charge separation (k_{CS}), rate constanst for charge recombination (k_{CR}), and charge-separated-state lifetimes(τ_{CS}) of ZnTPP and ZnP–(C=C)$_n$–C$_{60}$.

Compound	Solvent	Φ_f ZnP	k_{CS} [s^{-1}][a]	k_{CS} [s^{-1}][b]	k_{CR} [s^{-1}]	τ_{CS} [ns]
9 ($n=2$)	toluene	0.6×10^{-3}	2.1×10^{10}[c]	–	–	–
	THF	0.5×10^{-3}	2.6×10^{10}	1.1×10^{10}	1.8×10^{6}	555
	PhCN	0.4×10^{-3}	3.3×10^{10}	2.3×10^{10}	3.1×10^{6}	322
10 ($n=3$)	toluene	0.9×10^{-3}	1.4×10^{10}[c]	–	–	–
	THF	0.8×10^{-3}	1.6×10^{10}	7.3×10^{9}	1.6×10^{6}	625
	PhCN	0.6×10^{-3}	2.2×10^{10}	1.1×10^{10}	2.3×10^{6}	435
11 ($n=4$)	toluene	1.6×10^{-3}	0.8×10^{10}[c]	–	–	–
	THF	1.1×10^{-3}	1.1×10^{10}	5.5×10^{9}	1.4×10^{6}	714
	PhCN	0.9×10^{-3}	1.4×10^{10}	7.8×10^{9}	1.9×10^{6}	526

[a] Extrapolated from fluorescence experiments. [b] Determined from femto/picosecond transient absorption measurements. [c] Energy transfer.

700 nm), similar to what is depicted in Figure 13. The high triplet quantum yields (>90%) for these dyads in toluene confirm that quenching of ^{1}ZnP* occurs by singlet–singlet energy transduction.

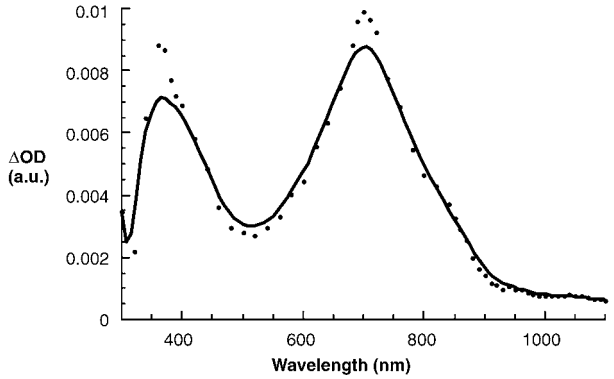

Figure 13. Differential absorption spectrum (visible and near-infrared) obtained upon nanosecond flash photolysis (532 nm) of $\sim 1.0\times10^{-5}$ M solutions of ZnP–(acetylene)$_4$–C_{60} in nitrogen-saturated toluene with a time delay of 100 ns at room temperature. The spectrum corresponds to ZnP–(C=C)$_4$–$^3C_{60}$*.

The transient absorption changes of the dyads in THF and PhCN were measured with several time delays after the 532 nm picosecond laser pulse, and were compared with the behavior of ZnTPP under the same conditions. At early times (20–50 ps), the spectra of the dyads are practically identical to those of ZnTPP, with strong bleaching at 550 nm, attesting to the formation of ^{1}ZnP*. After a delay time of approximately 100 ps, a new transition around 640 nm starts to grow in with the dyads, as seen in Figure 14 for compound **11**. This is accompanied by appearance of absorption in the near-infrared (NIR) region near 1000 nm, complete within 2000 ps. Based on spectral comparisons, the former is ascribed to the zinc–porphyrin π radical cation

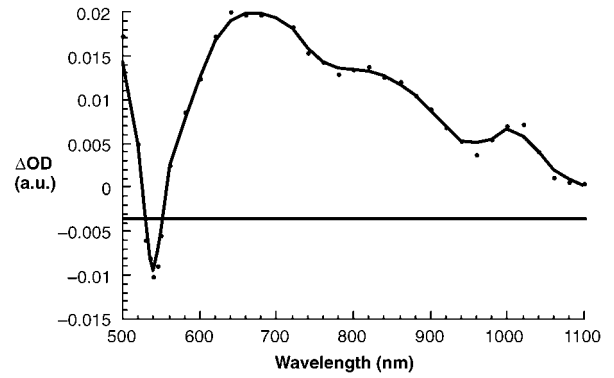

Figure 14. Differential absorption spectrum (visible and near-infrared) obtained upon nanosecond flash photolysis (532 nm) of $\sim 1.0\times10^{-5}$ M solutions of ZnP–(acetylene)$_4$–C_{60} in nitrogen-saturated THF with a time delay of 100 ns at room temperature. The spectrum corresponds to the radical pair, ZnP$^{\bullet+}$–(C=C)$_4$–[C_{60}]$^{\bullet-}$.

(ZnP$^{\bullet+}$), while the latter is due to fullerene π radical anions ($C_{60}^{\bullet-}$).[2a–c,e–g,i–k] Important criteria are the kinetic resemblance 1) between the decay of ^{1}ZnP* and the growth of ZnP$^{\bullet+}$/$C_{60}^{\bullet-}$, and 2) between the decay/growth kinetics and the fluorescence lifetimes. The rates of charge separation for **9** in THF and PhCN determined by this technique are 1.1×10^{10} and 2.3×10^{10} s^{-1}, respectively. The rates for **11** are slightly slower, with values of 5.5×10^9 s^{-1} in THF and 7.8×10^9 s^{-1} in PhCN. Good agreement was found with the data obtained from the steady-state fluorescence measurements.

From these results, we propose that charge separation from the ^{1}ZnP* to the electron-accepting fullerene in polar solvents directly affords ZnP$^{\bullet+}$/$C_{60}^{\bullet-}$, bypassing $^1C_{60}$*. The absorption of the charge-separated radical pair (CSRP) ZnP$^{\bullet+}$/$C_{60}^{\bullet-}$ is persistent on the picosecond timescale and decays in the nano- to microsecond range (vide infra).

Charge-recombination dynamics were analyzed by following the absorption decay of the reduced form of the electron acceptor ($C_{60}^{\bullet-}$) and of the oxidized form of the electron donor (ZnP$^{\bullet+}$). In oxygen-free solutions, the decays could be fitted well to a single-exponential expression. As seen in Table 2, the lifetimes of the charge-separated states for **9**, **10**, and **11** were longer in THF than in PhCN: **9**, 555 ns in THF, 322 ns in PhCN; **10**, 625 ns in THF, 435 ns in PhCN; **11**, 714 ns in THF, 526 ns in PhCN.

Finally, a plot of the back-electron transfer rates as a function of donor–acceptor separation led to a distance dependence from which we determined attenuation factors (β) of 0.06 ± 0.005 Å^{-1} (see Figure 15). This "wirelike" behavior signifies effective π conjugation between the phenyl group of the porphyrin donor, the polyacetylene bridge, and the fullerene.

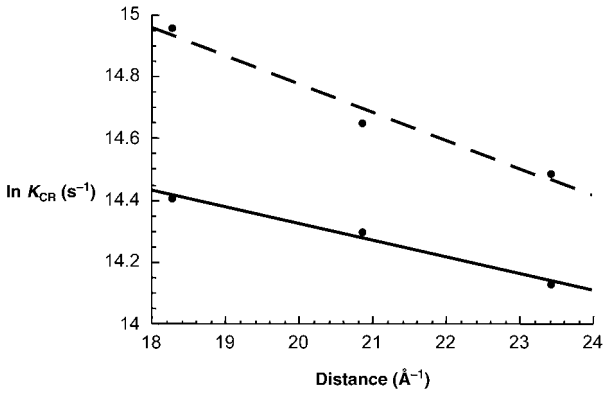

Figure 15. Center-to-center distance dependence of ET rate constants in ZnP–(acetylene)$_n$–C_{60} in nitrogen-saturated THF (——) and benzonitrile (– – –) at room temperature.

Discussion

In the present study, a series of ZnP–(acetylene)$_n$–C_{60} dyads (**9**, **10**, and **11**) were synthesized to assess the ability of polyalkynyl linkers to facilitate energy transduction and ET in ZnP–C_{60} "molecular-wire" systems. Although a small red-

shift was observed in the UV-visible absorption spectrum of each dyad relative to its zinc–porphyrin component, the optical spectra did not indicate substantial ground-state interaction between the chromophores.

Cyclic voltammetry (CV) and differential pulse voltammetry (DPV) measurements were also performed to determine the degree of electronic coupling between the ZnP and C_{60} moieties within the series. The TMS-terminated zinc–porphyrins (**3**, **5**, and **7**) show more positive reduction potentials than the H-terminated analogues (**4**, **6**, and **8**). The changes in the reduction potentials of the D–A dyads **9**, **10**, and **11** compared with model compounds show that the ZnP (donor) and C_{60} (acceptor) are indeed electronically coupled to some extent. The effect of increasing the number of spacer units on the first reduction potentials indicates that the electronic coupling between the porphyrin and the fullerene moieties decreases with increasing separation, as expected. The coupling, however, is not sufficient to cause major changes in the electronic absorption and emission spectra of the dyads.

Steady-state fluorescence measurements on dyads **9**, **10**, and **11** showed strong quenching of the zinc–porphyrin fluorescence in the dyads relative to ZnTPP in all solvents. The observed quenching behavior reflects a weak distance dependence. C_{60} fluorescence, observed at ~715 nm for the ZnP–(acetylene)$_n$–C_{60} dyads in toluene, is suggestive of a rapid intramolecular transduction of singlet excitation, supported by transient absorption studies clearly demonstrating formation of $^3C_{60}$*. The high fullerene triplet quantum yields confirm that transduction of singlet excitation in toluene is taking place.

The ZnP fluorescence decays for **11** in THF and PhCN indicate increasingly faster deactivation as the solvent polarity is increased, consistent with an intramolecular ET mechanism. Transient absorption measurements for **9**, **10**, and **11** in THF and PhCN, at short time delays, together with strong bleaching of ZnP absorption at 550 nm, are consistent with initial generation of ^{1}ZnP*, which undergoes rapid ET to directly give charge-separated radical pairs, $ZnP^{\bullet+}/C_{60}^{\bullet-}$. The $ZnP^{\bullet+}/C_{60}^{\bullet-}$ absorption in turn decays in the nano-/microsecond range. The lack of C_{60} fluorescence in THF and PhCN is another strong indication that ET is occurring, rather than the EnT process observed in toluene.

The rate of CR, as measured by the decay of $ZnP^{\bullet+}$ and $C_{60}^{\bullet-}$ in the transient absorption spectra, was faster in PhCN than in THF (Table 2). A decrease in $-\Delta G°$, accompanied by faster CR kinetics, is a phenomenon typically observed for back-electron transfer in the Marcus inverted region, where ET rates (k_{ET}) decrease with an increase in the thermodynamic driving force. The mechanism for charge separation can be explained in terms of an electron superexchange mechanism leading directly to the radical ion pair, as determined by the large LUMO(ZnP)–LUMO(wire) gap of greater than 0.3 eV. Alternatively, CR may proceed through an ET or hole-transfer pathway. The existence of a large LUMO(C_{60})–LUMO(wire) gap of at least 1.0 eV[41] is indicative of an electron-tunneling mechanism as the dominant reaction pathway. Hole transfer from the HOMO(C_{60}) to the HOMO(ZnP) could proceed through a superexchange or electron-hopping mechanism. As electron hopping is unlikely to occur under the experimental conditions at room temperature, a superexchange mechanism is proposed as the operative mode. Currently, we are focusing our research on establishing the relationship between superexchange and electron-hopping mechanisms in this series of conjugated donor–acceptor hybrids.

A small attenuation factor (β) of 0.06 ± 0.005 Å^{-1} was calculated from the plot in Figure 15 of ET rates in dyads **9**–**11** as a function of D–A distances, determined by molecular modeling (see Figure S11, Supporting Information). The exceptional "wirelike" behavior observed in dyads **9**–**11** can be rationalized in terms of the full π conjugation achieved between the phenyl ring of the porphyrin donor, the polyacetylene linker, and the C_{60} moiety.

Conclusion

Enhanced ET and EnT phenomena have previously been reported in highly conjugated porphyrin arrays linked by alkyne bridges.[42] Strong electronic coupling and rapid photoinduced ET phenomena were observed in analogous porphyrin donor–acceptor systems with a Zn^{II}-porphyrin donor and Au^{III}-porphyrin acceptor.[43] The D–bridge–A systems described in this work represent the first examples of *fully* conjugatively linked ZnP–C_{60} dyads, in which π conjugation extends the entire length of the bridge connecting the zinc–porphyrin to the fullerene sphere. These systems exhibit very rapid CS and somewhat slower CR dynamics in polar solvents, and singlet–singlet energy transfer in nonpolar solvents. Cyclic and differential pulse voltammetry measurements have shown that the ZnP and C_{60} components are electronically coupled, probably due to a combination of conjugative and weak donor–acceptor interactions, with the degree of interaction between the chromophores *decreasing* with increasing length of the alkynyl chain. This pattern of behavior following photoexcitation, namely EnT in nonpolar solvents and ET in polar solvents, is similar to that seen in several other types of covalently linked porphyrin fullerene dyads.[33,37,44] An increase in ET rates with increasing solvent polarity is consistent with normal Marcus behavior for charge separation. In contrast, the long CSRP lifetimes in THF, a polar solvent that lowers the energy of the CS state relative to the ground state, indicates that CR events are occurring in the Marcus inverted region.[2] Finally, the attenuation factors (β) of 0.06 ± 0.005 Å^{-1} are exceptionally small, relative to those observed for D–A systems with conjugated phenylene ($\beta = 0.32$–0.66 Å^{-1}),[14] polyene ($\beta = 0.04$–0.2 Å^{-1}),[15,16] and polyyne ($\beta = 0.04$–0.17 Å^{-1})[16b,17] linkers, but somewhat larger than those obtained for wires incorporating exTTF as the electron donor and C_{60} as the acceptor ($\beta = 0.01 \pm 0.005$ Å^{-1}).[18] These results support the conclusion that polyacetylene linkers with sp carbons are highly ef-

fective mediators of electronic interaction between porphyrin and fullerene moieties in conjugated D–A assemblies

Experimental Section

General: All commercially available reagents were used as received unless noted otherwise. Anhydrous toluene (containing $<0.001\,\%$ water) was purchased from Aldrich and was used as received. Tetrahydrofuran (THF) was freshly distilled over potassium, with benzophenone as indicator, prior to use. Methylene chloride was dried by distillation over sodium metal and was used immediately after distillation. Preparative thin-layer chromatography was performed using TLC standard grade silica gel (Aldrich), with gypsum binder (particle size 2–25 μ, BET surface area $\sim 500\ m^2g^{-1}$, pore volume $0.75\ cm^3g^{-1}$, average pore diameter 60 Å). All ^{1}H NMR spectra were obtained on Bruker-AV 400 MHz and Varian 200 MHz NMR spectrometers with TMS as an internal standard. Mass spectra for all samples were obtained using a Bruker Daltronics MALDI-TOF mass spectrometer. Mass calibrations were performed using tetra[3,5-di(*tert*-butyl)phenyl]porphine for compounds **3–8** and pristine C_{60} for compounds **1**, **2**, and **9–11**. All UV/Vis measurements were performed on a Hewlett–Packard 8453 UV/Vis spectrophotometer. Molecular modeling calculations for ZnP–C_{60} dyads **9**, **10**, and **11** were performed using Spartan (MMFF94 force field), with energy-minimized conformations. All oxidative coupling reactions were performed in one-neck round-bottomed flasks equipped with a calcium sulfate drying tube, and protected from light.

1-Trimethylsilylethynyl-2-methyl[60]fullerene (1): Lithium trimethylsilylacetylide (1.8 mL, 0.9 mmol) was added to a deoxygenated solution of C_{60} (200 mg, 0.28 mmol) in anhydrous toluene (220 mL), under vigorous stirring. The mixture was stirred at room temperature for about 1.5 h under an argon atmosphere. To the mixture, iodomethane (0.2 mL, 0.32 mmol) was added and then dry THF (50 mL). The mixture was heated at 40 °C for 3 h. The reaction mixture was filtered through a silica-gel column using toluene as the eluent. The product was purified on a silica column using hot cyclohexane as the eluent to afford **1** as a brown solid (50 %). ^{1}H NMR (200 MHz, $CDCl_3$, 25 °C): $\delta = 0.44$ (s, 9H; $(CH_3)_3Si$), 3.43 ppm (s, 3H; CH_3); MALDI-TOF: calcd for $C_{66}H_{12}Si$ [M^+]: 832.07; found: 832.99 [M^+], 817.92 [M^+-CH_3], 720.64 [C_{60}^+].

1-Ethynyl-2-methyl[60]fullerene (2): Potassium carbonate (50 mg) was added to a solution of **1** (80 mg, 0.096 mmol) in THF (120 mL) and MeOH (24 mL). The reaction vessel was flushed with argon for 10–15 min at room temperature with vigorous stirring and was heated at reflux for about 3–4 h. The mixture was cooled and filtered through a silica funnel using CS_2 as eluent. The solvent was removed under reduced pressure and the crude product was chromatographed on silica with cyclohexane as the eluent to afford **2** as a brown solid (45 %). ^{1}H NMR (200 MHz, $CDCl_3$, 25 °C): $\delta = 3.06$ (s, 1H; CC–H), 3.49 ppm (s, 3H; CH_3); MALDI-TOF: calcd for $C_{63}H_4$ [M^+]: 760.03; found: 758.9 [M^+], 743.46 [M^+-CH_3], 718.28 [C_{60}^+].

Zinc(II)–5-[4-(trimethylsilylethynyl)phenyl]-10,15,20-tris[3,5-di(*tert*-butyl)phenyl]porphine (3): Pyrrole (2 mL) was added through a dropping funnel to a solution of 3,5-di(*tert*-butyl)benzaldehyde (4.7 g, 21 mmol) and 4-(trimethylsilylethynyl)benzaldehyde (1.8 g, 8.8 mmol) in refluxing glacial acetic acid (200 mL) and nitrobenzene (120 mL). The mixture was heated at reflux for 1 h, stirred overnight at room temperature, followed by vacuum distillation to remove the solvents from the reaction vessel. The mixture was cooled, washed with methanol, and filtered through a silica funnel with CH_2Cl_2 as eluent. To a solution of the crude porphyrin mixture in $CHCl_3$ (250 mL) and methanol (125 mL), $Zn(OAc)_2{\cdot}2H_2O$ (5.0 g) was added. The mixture was heated at reflux for 4 h, cooled, filtered, concentrated, and chromatographed on silica gel with hexanes/CH_2Cl_2 (4:1) to afford a purple, crystalline solid in 16 % overall yield. ^{1}H NMR (400 MHz, $CDCl_3$, 25 °C): $\delta = 0.38$ (s, 9H; Si–CH_3), 1.52 (m, 54H; *t*Bu–H), 7.79 (s, 3H; *p*-*t*BuPh–H), 7.86 (d, 2H; *m*-H–PhCCTMS), 8.08 (s, 6H; *o*-*t*BuPh–H), 8.18 (d, 2H; *o*-H–PhCCTMS), 8.91 (d, 2H; pyrrole–H), 9.00 ppm (d, 6H; pyrrole–H); UV/Vis ($CHCl_3$): λ_{max} ($\varepsilon \times 10^3$) = 423 (136), 550 (5.50), 596 nm ($1.68\ mol^{-1}dm^3cm^{-1}$); MALDI-TOF: calcd for $C_{73}H_{84}N_4SiZn$ [M^+]: 1108.58; found: 1108.75.

Zinc(II)–5-(4-ethynylphenyl)-10,15,20-tris[3,5-di(*tert*-butyl)phenyl]porphine (4): TBAF (4 mmol) was added to a solution of **3** (240 mg, 0.22 mmol) in THF (32 mL) with vigorous stirring. After 15 min, glacial acetic acid (1 mL) was added and the reaction mixture was filtered through a silica funnel using CH_2Cl_2 as eluent to afford **5** as a purple, crystalline solid (99 %). ^{1}H NMR (400 MHz, $CDCl_3$, 25 °C): $\delta = 1.53$ (m, 54H; *t*Bu–H), 3.30 (s, 1H; PhCCH), 7.79 (s, 3H; *p*-*t*BuPh–H), 7.84 (d, 2H; *m*-H–PhCCH), 8.09 (s, 6H; *o*-*t*BuPh–H), 8.21 (d, 2H; *o*-H–PhCCH), 8.92 (d, 2H; pyrrole–H), 9.00 ppm (d, 6H; pyrrole–H); UV/Vis ($CHCl_3$): λ_{max} ($\varepsilon \times 10^3$) = 423 (133), 551 (5.22), 592 nm ($1.50\ mol^{-1}dm^3cm^{-1}$); MALDI-TOF: calcd for $C_{70}H_{76}N_4Zn$ [M^+]: 1036.54; found: 1036.735.

Zinc(II)–5-[4-(trimethylsilylbutadiynyl)phenyl]-10,15,20-tris[3,5-di(*tert*-butyl)phenyl]porphine (5): Trimethylsilylacetylene (0.7 mL, 2 mmol) and CuCl (300 mg) were added to a solution of **4** (200 mg, 0.2 mmol) in dry methylene chloride (250 mL). The mixture was stirred vigorously under a dry oxygen atmosphere for 2 h followed by dropwise addition of TMEDA (2 mL). The reaction mixture was vigorously stirred for 1.5–2 h under a dry oxygen atmosphere and was filtered through a silica funnel to remove any insoluble residue. The solvent was removed under reduced pressure and the crude porphyrin was redissolved in hexanes and transferred onto a silica funnel. The porphyrin was washed thoroughly on the funnel with hexanes and then eluted with chloroform. The solvent was removed under reduced pressure to afford **6** as a purple crystalline solid in quantitative yield (as evidenced by TLC). ^{1}H NMR (400 MHz, $CDCl_3$, 25 °C): $\delta = 0.32$ (s, 9H; Si–CH_3), 1.52 (m, 54H; *t*Bu–H), 7.79 (s, 3H; *p*-*t*BuPh–H), 7.88 (d, 2H; *m*-H–PhCCTMS), 8.08 (s, 6H; *o*-*t*BuPh–H), 8.20 (d, 2H; *o*-H–PhCCTMS), 8.90 (d, 2H; pyrrole–H), 9.00 ppm (d, 6H; pyrrole–H); UV/Vis ($CHCl_3$): λ_{max} ($\varepsilon \times 10^3$) = 425 (136), 551 (5.50), 593 nm ($1.65\ mol^{-1}dm^3cm^{-1}$); MALDI-TOF: calcd for $C_{75}H_{84}N_4SiZn$ [M^+]: 1132.58; found: 1132.85.

Zinc(II)–5-(4-butadiynylphenyl)-10,15,20-tris[3,5-di(*tert*-butyl)phenyl]porphine (6): TBAF (4 mmol) was added to a solution of **5** (190 mg, 0.17 mmol) in THF (40 mL) with vigorous stirring. After 15 min, glacial acetic acid (1 mL) was added and the reaction mixture was filtered through a silica funnel using CH_2Cl_2 as eluent to afford **6** as a purple crystalline solid (97 %). ^{1}H NMR (400 MHz, $CDCl_3$, 25 °C): $\delta = 1.53$ (m, 54H; *t*Bu–H), 2.59 (s, 1H; PhCCH), 7.79 (s, 3H; *p*-*t*BuPh–H), 7.91 (d, 2H; *m*-H–PhCCH), 8.08 (s, 6H; *o*-*t*BuPh–H), 8.22 (d, 2H; *o*-H–PhCCH), 8.90 (d, 2H; pyrrole–H), 9.01 ppm (d, 6H; pyrrole–H); UV/Vis ($CHCl_3$): λ_{max} ($\varepsilon \times 10^3$) = 424 (135), 551 (5.46), 592 nm ($1.65\ mol^{-1}dm^3cm^{-1}$); MALDI-TOF: calcd for $C_{72}H_{76}N_4Zn$ [M^+]: 1060.54; found: 1060.94.

Zinc(II)–5-[4-(trimethylsilylhexatriynyl)phenyl]-10,15,20-tris[3,5-di(*tert*-butyl)phenyl]porphine (7): Trimethylsilylacetylene (0.5 mL, 1.4 mmol) and CuCl (200 mg) were added to a solution of **6** (100 mg, 0.1 mmol) in dry methylene chloride (250 mL). The mixture was stirred vigorously under a dry oxygen atmosphere for 2 h followed by dropwise addition of TMEDA (1 mL). The reaction mixture was vigorously stirred for 1.5–2 h under dry oxygen and was filtered through a silica funnel to remove any insoluble residue. The solvent was removed under reduced pressure and the crude porphyrin was redissolved in hexanes and transferred onto a silica funnel. The porphyrin was washed thoroughly on the funnel with hexanes and then eluted with chloroform. The solvent was removed under reduced pressure to afford **7** as a purple crystalline solid in quantitative yield (as evidenced by TLC). ^{1}H NMR (400 MHz, $CDCl_3$, 25 °C): $\delta = 0.27$ (s, 9H; Si–CH_3), 1.51 (m, 54H; *t*Bu–H), 7.79 (s, 3H; *p*-*t*BuPh–H), 7.91 (d, 2H; *m*-H–PhCCTMS), 8.08 (s, 6H; *o*-*t*BuPh–H), 8.21 (d, 2H; *o*-H–PhCCTMS), 8.89 (d, 2H; pyrrole–H), 9.00 ppm (d, 6H; pyrrole–H); UV/Vis ($CHCl_3$): λ_{max} ($\varepsilon \times 10^3$) = 425 (136), 551 (6.00), 592 nm ($2.18\ mol^{-1}dm^3cm^{-1}$); MALDI-TOF: calcd for $C_{77}H_{84}N_4SiZn$ [M^+]: 1156.58; found: 1156.90.

Zinc(II)–5-(4-hexatriynylphenyl)-10,15,20-tris[3,5-di(*tert*-butyl)phenyl]-porphine (8): TBAF (4 mmol) was added to a solution of **7** (100 mg, 0.09 mmol) in THF (25 mL) with vigorous stirring. After 15 min, glacial acetic acid (0.5 mL) was added and the reaction mixture was filtered

through a silica funnel using CH_2Cl_2 as eluent to afford **8** as a purple crystalline solid (96%). ^{1}H NMR (400 MHz, $CDCl_3$, 25°C): $\delta = 1.52$ (m, 54H; *t*Bu–H), 2.27 (s, 1H; PhCCH), 7.79 (s, 3H; *p*-*t*BuPh–H), 7.90 (d, 2H; *m*-H–PhCCH), 8.08 (s, 6H; *o*-*t*BuPh–H), 8.22 (d, 2H; *o*-H–PhCCH), 8.90 (d, 2H; pyrrole–H), 8.98 ppm (d, 6H; pyrrole–H); UV/Vis ($CHCl_3$): λ_{max} ($\varepsilon \times 10^3$) = 424 (135), 550 (5.85), 591 nm (1.76 $mol^{-1} dm^3 cm^{-1}$); MALDI-TOF: calcd for $C_{74}H_{76}N_4Zn$ [M^+]: 1084.54; found: 1084.96.

Zinc(II)–5-(4-alkynylphenyl)-10,15,20-tris[3,5-di(*tert*-butyl)phenyl]porphine-1-ethynyl-2-methyl[60]fullerene dyads (9, 10, and 11)

General procedure: CuCl (208 mg, 2.1 mmol) and TMEDA (0.3 mL, 2 mmol) were added, under a dry oxygen atmosphere, to a solution of **2** (15 mg, 19.7 μM) and **4**, **6**, or **8** (9.6 μM) in chlorobenzene (30 mL) at room temperature. The reaction mixture was stirred at room temperature for 90 min and filtered through a silica funnel using CS_2 as eluent. The solvent was removed under reduced pressure and the crude product was dissolved in CS_2 and transferred onto a silica funnel. Separation of each ZnP–C_{60} dyad from the ZnP–ZnP and C_{60}–C_{60} homodimers was accomplished by eluting the silica funnel with copious amounts of CS_2. The ZnP–C_{60} dyads eluted before the ZnP–ZnP dimer, whereas the C_{60}–C_{60} dimer was permanently retained on the silica. Each dyad was further purified by preparative TLC on silica gel using CS_2 as eluent. Overall isolated yields for dyads **9**, **10**, and **11** were 29%, 26%, and 21%, respectively. The purity of **9**, **10**, and **11** was confirmed by TLC, ^{1}H NMR, and MALDI-TOF analysis. Elution with chloroform effectively isolated each of the corresponding ZnP–ZnP dimers, whose identities were confirmed by MALDI-TOF analysis; these materials were not otherwise characterized. The mass obtained for each of the ZnP–ZnP homodimers from the synthesis of **9**, **10**, and **11** were 2071.56 (calcd 2071.06), 2119.83 (calcd 2119.06) and 2168.14 (calcd 2167.06), respectively. The silica containing the C_{60}–C_{60} homodimer (i.e., the dimer of **2**) was sonicated in a flask containing CS_2, filtered, and concentrated to furnish the dimer in a very small quantity. Its identity was confirmed by MALDI-TOF analysis by a mass peak at 1518.92 (calcd 1518.05). It should be noted that the oxidative coupling protocol employed in the synthesis of dyads **9**, **10**, and **11** was complete with respect to the consumption of terminal alkyne starting material, resulting in a statistical distribution of homo- and heterodimers.

Dyad ***9***: ^{1}H NMR (400 MHz, $CDCl_3$, 25°C): $\delta = 1.45$ (m, 54H; *t*Bu–H), 2.83 (s, 3H; CH_3), 7.71 (s, 3H; *p*-*t*BuPh–H), 7.91 (s, 4H; *o*-*t*BuPh–H), 7.99 (s, 2H; *o*-*t*BuPh–H), 8.29 (d, 2H; *m*-H–PhCC), 8.50 (d, 2H; *o*-H–PhCC), 8.82 (d, 2H; β-$H_{13,17}$), 8.87 (d, 2H; β-$H_{12,18}$), 8.95 (d, 2H; β-$H_{2,8}$), 9.02 ppm (d, 2H; β-$H_{3,7}$); UV/Vis ($CHCl_3$): λ_{max} ($\varepsilon \times 10^3$) = 258 (54.4), 424 (134), 551 (6.34), 592 nm (2.42 $mol^{-1} dm^3 cm^{-1}$); MALDI-TOF: calcd for $C_{133}H_{78}N_4Zn$ [M^+]: 1794.55; found: 1794.89.

Dyad ***10***: ^{1}H NMR (400 MHz, $CDCl_3$, 25°C): $\delta = 1.45$ (m, 54H; *t*Bu–H), 2.74 (s, 3H; CH_3), 7.71 (s, 3H; *p*-*t*BuPh–H), 7.96 (s, 4H; *o*-*t*BuPh–H), 8.00 (s, 2H; *o*-*t*BuPh–H), 8.11 (d, 2H; *m*-H–PhCC), 8.34 (d, 2H; *o*-H–PhCC), 8.86–9.0 ppm (m, 8H; pyrrole–H); UV/Vis ($CHCl_3$): λ_{max} ($\varepsilon \times 10^3$) 258 (59.3), 424 (130), 551 (6.37), 593 nm (2.44 $mol^{-1} dm^3 cm^{-1}$); MALDI-TOF: calcd for $C_{135}H_{78}N_4Zn$ [M^+]: 1818.55; found 1818.86.

Dyad ***11***: ^{1}H NMR (400 MHz, $CDCl_3$, 25°C): $\delta = 1.41$ (m, 54H; *t*Bu–H), 2.32 (s, 3H; CH_3), 7.72 (s, 3H; *p*-*t*BuPh–H), 8.00 (d, 6H; *o*-*t*BuPh–H), 8.09 (d, 2H; *m*-H–PhCC), 8.26 (d, 2H; *o*-H–PhCC), 8.93 (m, 8H; pyrrole–H), 9.05 ppm; UV/Vis ($CHCl_3$): λ_{max} ($\varepsilon \times 10^3$) = 258 (56.5), 425 (136), 551 (6.40), 593 nm (2.50 $mol^{-1} dm^3 cm^{-1}$); MALDI-TOF: calcd for $C_{137}H_{78}N_4Zn$ [M^+]: 1842.55; found: 1842.65.

Cyclic voltammetry: The electrochemical measurements for compounds **2**–**8** were performed using a CHI 440 Electrochemical Workstation (CH Instruments Inc., Austin, Texas). Tetrabutylammonium hexafluorophosphate (Fluka) in redistilled CH_2Cl_2 (0.1 M) was used as the supporting electrolyte (degassed with argon and saturated with CH_2Cl_2 vapors). A platinum wire was employed as the counter electrode and a nonaqueous Ag/AgCl electrode was used as the reference. Ferrocene (Fc) was added as an internal reference and all the potentials were referenced relative to the Fc/Fc^+ couple. A glassy carbon electrode (CHI, 1.5 mm in diameter), polished with aluminum paste (0.3 μm) and ultrasonicated in a deionized water and CH_2Cl_2 bath, was used as the working electrode. The scan rates for cyclic voltammetry were 100 mV and the pulse rate was set at 0.05 s at increments of 4 mV and an amplitude of 50 mV for the differential pulse voltammetry measurements. All experiments were performed at room temperature (20±2°C).

Due to limited sample availability, compounds **9**, **10**, and **11** were studied in a special cell similar to one described earlier.[45,46] This assembly consists of a glass tube (1.5 mm diameter) fitted with a vycor tip (working volume of 100 μL) and contained the test solution (compound + $TBAPF_6$ in CH_2Cl_2). This cell was immersed in a glass vial containing the electrolyte solution. A platinum wire was employed as the counter electrode and a nonaqueous Ag/AgCl electrode was used as the reference. This electrode was similarly immersed in the electrolyte contained in the outside glass vial.

Spectroscopic measurements: Picosecond laser flash photolysis experiments were performed using 355 or 532 nm laser pulses from a mode-locked, Q-switched Quantel YG-501 DP Nd:YAG laser system (18 ps pulse width, 2–3 mJ $pulse^{-1}$). Nanosecond laser flash photolysis experiments were performed with 355 or 532 nm laser pulses from a Quanta-Ray CDR Nd:YAG system (6 ns pulse width) in a front-face excitation geometry.

Fluorescence lifetimes were measured with a Laser Strobe Fluorescence Lifetime Spectrometer (Photon Technology Int.) with 337 nm laser pulses from a nitrogen laser fiber coupled to a lens-based T-formal sample compartment equipped with a stroboscopic detector. Details of the laser strobe systems are described on the manufacturer's web site, http://www.pti-nj.com.

Emission spectra, all measured at room temperature, were recorded on a SLM 8100 Spectrofluorometer. Each spectrum represents an average of at least five individual scans, with appropriate corrections when necessary.

Acknowledgements

The NYU group is grateful to the National Science Foundation for support of this research under grant CHE-0097089. The electrochemical studies at Clemson were also supported by the National Science Foundation. J.P.C.T. thanks Professor José Cavaleiro and the University of Aveiro, Portugal, for a special postdoctoral fellowship that allowed him to spend a summer at NYU. Photophysical studies by D.M.G. at Notre Dame were supported by the U.S. Department of Energy. We also gratefully acknowledge grant MRI-0116222 from the National Science Foundation for the purchase of new NMR spectrometers at NYU.

[1] H. Kurreck, M. Huber, *Angew. Chem.* **1995**, *107*, 929–947; *Angew. Chem. Int. Ed. Engl.* **1995**, *34*, 849–866.

[2] a) P. A. Liddell, D. Kuciauskas, J. P. Sumida, B. Nash, D. Nguyen, A. L. Moore, T. A. Moore, D. Gust, *J. Am. Chem. Soc.* **1997**, *119*, 1400–1405; b) D. M. Guldi, M. Prato, *Acc. Chem. Res.* **2000**, *33*, 695–703; c) C. Luo, D. M. Guldi, H. Imahori, K. Tamaki, Y. Sakata, *J. Am. Chem. Soc.* **2000**, *122*, 6535–6551; d) H. Imahori, K. Tamaki, H. Yamada, K. Yamada, Y. Sakata, Y. Nishimura, I. Yamazaki, M. Fujitsuka, O. Ito, *Carbon* **2000**, *38*, 1599–1605; e) H. Imahori, M. E. El-Khouly, M. Fujitsuka, O. Ito, Y. Sakata, S. Fukuzumi, *J. Phys. Chem. A* **2001**, *105*, 325–332; f) H. Imahori, K. Tamaki, D. M. Guldi, C. Luo, M. Fujitsuka, O. Ito, Y. Sakata, S. Fukuzumi, *J. Am. Chem. Soc.* **2001**, *123*, 2607–2617; g) H. Imahori, D. M. Guldi, K. Tamaki, Y. Yoshida, C. Luo, Y. Sakata, S. Fukuzumi, *J. Am. Chem. Soc.* **2001**, *123*, 6617–6628; h) S. Fukuzumi, K. Ohkubo, H. Imahori, D. M. Guldi, *Chem. Eur. J.* **2003**, *9*, 1585–1593; i) Y. Kashiwagi, K. Ohkubo, J. A. McDonald, I. M. Blake, M. J. Crossley, Y. Araki, O. Ito, H. Imahori, S. Fukuzumi, *Org. Lett.* **2003**, *5*, 2719–2721; j) K. Ohkubo, H. Kotani, J. Shao, Z. Ou, K. M. Kadish, G. Li, R. K. Pandey, M. Fujitsuka, O. Ito, H. Imahori, S. Fukuzumi, *Angew. Chem.* **2004**, *116*, 871–874; *Angew. Chem. Int. Ed.* **2004**, *43*, 853–856; k) H. Imahori, Y. Sekiguchi, Y. Kashiwagi, T. Sato, Y. Araki, O. Ito, H. Yamada, S. Fukuzumi, *Chem. Eur. J.* **2004**, *10*, 3184–3196.

[3] a) N. Martin, L. Sanchez, B. Illescas, I. Pérez, *Chem. Rev.* **1998**, *98*, 2527–2547; b) H. Imahori, H. Norieda, H. Yamada, Y. Nishimura, I. Yamazaki, Y. Sakata, S. Fukuzumi, *J. Am. Chem. Soc.* **2001**, *123*, 100–110; c) A. Ikeda, T. Hatano, S. Shinkai, T. Akiyama, S. Yamada, *J. Am. Chem. Soc.* **2001**, *123*, 4855–4856; d) F. Fungo, L. Otero, C. D. Borsarelli, E. N. Durantini, J. J. Silber, L. Sereno, *J. Phys. Chem. B* **2002**, *106*, 4070–4078; e) H. Yamada, H. Imahori, S. Fukuzumi, *J. Mater. Chem.* **2002**, *12*, 2034–2040; f) H. Yamada, H. Imahori, Y. Nishimura, I. Yamazaki, T. K. Ahn, S. K. Kim, D. Kim, S. Fukuzumi, *J. Am. Chem. Soc.* **2003**, *125*, 9129–9139; g) S. N. Smirnov, P. Liddell, I. V. Vlassiouk, A. Teslja, D. Kuciauskas, C. L. Braun, A. L. Moore, T. A. Moore, D. Gust, *J. Phys. Chem. A* **2003**, *107*, 7567–7573; h) I. Zilbermann, G. A. Anderson, D. M. Guldi, H. Yamada, H. Imahori, S. Fukuzumi, *J. Porphyrins Phthalocyanines* **2003**, *7*, 357–364; i) D. M. Guldi, I. Zilbermann, G. A. Anderson, K. Kordatos, M. Prato, R. Tafuro, L. Valli, *J. Mater. Chem.* **2004**, *14*, 303–309; j) H. Imahori, Y. Kashiwagi, T. Hasobe, M. Kimura, T. Hanada, Y. Nishimura, I. Yamazaki, Y. Araki, O. Ito, S. Fukuzumi, *Thin Solid Films* **2004**, *451–452*, 580–588; k) D. M. Guldi, H. Imahori, K. Tamaki, Y. Kashiwagi, H. Yamada, Y. Sakata, S. Fukuzumi, *J. Phys. Chem. A* **2004**, *108*, 541–548; l) H. Imahori, S. Fukuzumi, *Adv. Funct. Mater.* **2004**, *14*, 525–536.

[4] a) H. M. Mc Connell, *J. Chem. Phys.* **1961**, *35*, 508–515; b) P. F. Barbara, T. J. Meyer, J. Ratner, *J. Phys. Chem.* **1996**, *100*, 13148–13168; c) N. Robertson, C. A. McGowan, *Chem. Soc. Rev.* **2003**, *32*, 96–103.

[5] a) J. M. Tour, *Adv. Mater.* **1994**, *6*, 190–197; b) J. M. Tour, *Chem. Rev.* **1996**, *96*, 537–553; c) R. E. Martin, F. Diederich, *Angew. Chem.* **1999**, *111*, 1440–1469; *Angew. Chem. Int. Ed.* **1999**, *38*, 1350–1377; d) J. Roncali, *Acc. Chem. Res.* **2000**, *33*, 147–156; e) J. M. Tour, *Acc. Chem. Res.* **2000**, *33*, 791–804; f) J. L. Segura, N. Martín, *J. Mater. Chem.* **2000**, *10*, 2403–2435; g) T. Otsubo, Y. Aso, K. Takimiya, *Bull. Chem. Soc. Jpn.* **2001**, *74*, 1789–1801; h) M. Fox, *Acc. Chem. Res.* **1999**, *32*, 201–207.

[6] a) H. Nakanishi, N. Sumi, Y. Aso, T. Otsubo, *J. Org. Chem.* **1998**, *63*, 8632–8633; b) H. Nakanishi, Y. Aso, T. Otsubo, *Synth. Met.* **1999**, *101*, 604–605; c) N. Sumi, H. Nakanishi, S. Ueno, K. Takimiya, Y. Aso, T. Otsubo, *Bull. Chem. Soc. Jpn.* **2001**, *74*, 979–988; d) H. Nakanishi, N. Sumi, S. Ueno, K. Takimiya, Y. Aso, T. Otsubo, K. Komaguchi, M. Shiotani, N. Ohta, *Synth. Met.* **2001**, *119*, 413–414.

[7] M. G. Harrison, R. H. Friend, *Electronic Materials: The Oligomer Approach*, Wiley-VCH, Weinheim, **1998**, pp. 515–558.

[8] a) Y. Shirota, *J. Mater. Chem.* **2000**, *10*, 1–25; b) U. Mitschke, P. Bäuerle, *J. Mater. Chem.* **2000**, *10*, 1471–1507.

[9] a) R. A. Hann, D. Bloor, *Organic Materials for Nonlinear Optics*, Royal Society of Chemistry, London, **1989**; b) C. Rubeck, *Electronic Materials: The Oligomer Approach*, Wiley-VCH, Weinheim, **1998**, pp. 449–478; c) H. S. Nalwa in *Handbook of Organic Conductive Molecules and Polymers*, *Vol. 4* (Ed.: H. S. Nalwa), Wiley, Chichester, **1997**.

[10] a) F. Garnier in *Electronic Materials: The Oligomer Approach* (Eds.: K. Müllen, G. Wegner), Wiley-VCH, Weinheim, **1998**, pp. 559–584; b) G. Horowitz, *Adv. Mater.* **1998**, *10*, 365–377; c) G. Horowitz, *J. Mater. Chem.* **1999**, *9*, 2021–2026; d) H. E. Katz, Z. Bao, S. L. Gilat, *Acc. Chem. Res.* **2001**, *34*, 359–369; e) C. D. Dimitrakopoulos, P. R. Malenfant, *Adv. Mater.* **2002**, *14*, 99–117.

[11] B. Jiang, S. W. Yang, W. E. Jones, *Chem. Mater.* **1997**, *9*, 2031–2034.

[12] J. Ikemoto, K. Takimiya, Y. Aso, T. Otsubo, M. Fujitsuka, O. Ito, *Org. Lett.* **2002**, *4*, 309–311.

[13] a) B. A. Leland, A. D. Joran, P. M. Felker, J. J. Hopfield, A. H. Zewail, P. B. Dervan, *J. Phys. Chem.* **1985**, *89*, 5571–5573; b) H. Oevering, M. N. Paddon-Row, M. Heppener, A. M. Oliver, E. Cotsaris, J. W. Verhoeven, N. S. Hush, *J. Am. Chem. Soc.* **1987**, *109*, 3258–3269; c) M. D. Johnson, J. R. Miller, N. S. Green, G. L. Closs, *J. Phys. Chem.* **1989**, *93*, 1173–1176; d) H. O. Finklea, D. D. Hanshew, *J. Am. Chem. Soc.* **1992**, *114*, 3173–3181; e) B. Paulson, K. Pramod, P. Eaton, G. Closs, J. R. Miller, *J. Phys. Chem.* **1993**, *97*, 13042–13045; f) J. Xu, H. L. Li, Y. Zhang, *J. Phys. Chem.* **1993**, *97*, 11497–11500; g) M. T. Carter, G. K. Rowe, J. N. Richardson, L. M. Tender, R. H. Terrill, R. W. Murray, *J. Am. Chem. Soc.* **1995**, *117*, 2896–2899.

[14] a) A. Osuka, K. Maruyama, N. Mataga, T. Asahi, I. Yamazaki, N. Tamai, *J. Am. Chem. Soc.* **1990**, *112*, 4958–4959; b) A. Helms, D. Heiler, G. McLendon, *J. Am. Chem. Soc.* **1992**, *114*, 6227–6238; c) F. Barigelletti, L. Flamigni, M. Guardigli, A. Juris, M. Beley, S. Chodorowski-Kimmens, J. P. Collins, J. P. Sauvage, *Inorg. Chem.* **1996**, *35*, 136–142; d) B. Schlicke, P. Belser, L. De Cola, E. Sabbioni, V. Balzani, *J. Am. Chem. Soc.* **1999**, *121*, 4207–4214.

[15] a) S. Speiser, *Chem. Rev.* **1996**, *96*, 1953–1976; b) S. B. Sachs, S. P. Dudek, R. P. Hsung, L. R. Sita, J. F. Smalley, M. D. Newton, S. W. Feldberg, C. E. D. Chidsey, *J. Am. Chem. Soc.* **1997**, *119*, 10563–10564.

[16] a) A. C. Benniston, V. Goulle, A. Harriman, J.-M. Lehn, B. Marczinke, *J. Phys. Chem.* **1994**, *98*, 7798–7804; b) A. Osuka, N. Tanabe, S. Kawabata, I. Yamazaki, N. Nishimura, *J. Org. Chem.* **1995**, *60*, 7177–7185.

[17] a) V. Grosshenny, A. Harriman, R. Ziessel, *Angew. Chem.* **1995**, *107*, 1211–1214; *Angew. Chem. Int. Ed. Engl.* **1995**, *34*, 1100–1102; b) V. Grosshenny, A. Harriman, R. Ziessel, *Angew. Chem.* **1995**, *107*, 2921–2925; *Angew. Chem. Int. Ed. Engl.* **1995**, *34*, 2705–2708.

[18] F. Giacalone, J. L. Segura, N. Martín, D. M. Guldi, *J. Am. Chem. Soc.* **2004**, *126*, 5340–5341.

[19] S. A. Vail, J. P. C. Tomé, P. J. Krawczuk, A. Dourandin, V. Shafirovich, J. A. S. Cavaleiro, D. I. Schuster, *J. Phys. Org. Chem.* **2004**, *17*, 814–818.

[20] a) G. Leatherman, E. N. Durantini, D. Gust, T. A. Moore, A. L. Moore, S. Stone, Z. Zhou, P. Rez, Y. Z. Liu, S. M. Lindsay, *J. Phys. Chem. B* **1999**, *103*, 4006–4010; b) J. L. Bahr, D. Kuciauskas, P. A. Liddell, A. L. Moore, T. A. Moore, D. Gust, *Photochem. Photobiol.* **2000**, *72*, 598–611; c) W. B. Davis, M. A. Ratner, M. R. Wasielewski, *Chem. Phys.* **2002**, *281*, 333–346; d) F. Fungo, L. Otero, E. Durantini, W. J. Thompson, J. J. Silber, T. A. Moore, A. L. Moore, D. Gust, L. Sereno, *Phys. Chem. Chem. Phys.* **2003**, *5*, 469–475; e) E. A. Weiss, M. J. Ahrens, L. E. Sinks, A. V. Gusev, M. A. Ratner, M. R. Wasielewski, *J. Am. Chem. Soc.* **2004**, *126*, 5577–5584.

[21] a) G. L. Closs, J. R. Miller, *Science* **1988**, *240*, 440–447; b) M. D. Newton, *Chem. Rev.* **1991**, *91*, 767–792; c) S. E. Miller, A. S. Lukas, E. Marsh, P. Bushard, M. R. Wasielewski, *J. Am. Chem. Soc.* **2000**, *122*, 7802–7810; d) A. S. Lukas, P. J. Bushard, M. R. Wasielewski, *J. Phys. Chem. A* **2002**, *106*, 2074–2082; e) D. Gust, T. A. Moore, A. L. Moore, A. N. Macpherson, A. Lopez, J. M. DeGraziano, I. Gouni, E. Bittersmann, G. R. Seely, *J. Am. Chem. Soc.* **1993**, *115*, 11141–11152; f) P. A. Liddell, G. Kodis, L. de la Garza, J. L. Bahr, A. L. Moore, T. A. Moore, D. Gust, *Helv. Chim. Acta* **2001**, *84*, 2765–2783; g) G. Kodis, P. A. Liddell, L. de la Garza, A. L. Moore, T. A. Moore, D. Gust, *J. Mater. Chem.* **2002**, *12*, 2100–2108; h) J. Springer, G. Kodis, L. de La Garza, A. L. Moore, T. A. Moore, D. Gust, *J. Phys. Chem. A* **2003**, *107*, 3567–3575; i) H. Imahori, D. M. Guldi, K. Tamaki, Y. Yoshida, C. Luo, Y. Sakata, S. Fukuzumi, *J. Am. Chem. Soc.* **2001**, *123*, 6617–6628; j) H. Imahori, K. Tamaki, Y. Araki, Y. Sekiguchi, O. Ito, Y. Sakata, S. Fukuzumi, *J. Am. Chem. Soc.* **2002**, *124*, 5165–5174; k) H. Imahori, S. Cardoso, D. Tatman, S. Lin, L. Noss, G. R. Seely, L. Sereno, J. Chessa De Silber, T. A. Moore, D. Gust, *Photochem. Photobiol.* **1995**, *62*, 1009–1014; l) H. Imahori, K. Hagiwara, M. Aoki, T. Akiyama, S. Taniguchi, T. Okada, M. Shirakawa, Y. Sakata, *J. Am. Chem. Soc.* **1996**, *118*, 11771–11782; m) H. Imahori, K. Yamada, M. Hasegawa, S. Taniguchi, T. Okada, Y. Sakata, *Angew. Chem.* **1997**, *109*, 2740–2742; *Angew. Chem. Int. Ed. Engl.* **1997**, *36*, 2626–2629; n) H. Imahori, K. Tamaki, Y. Araki, T. Hasobe, O. Ito, A. Shimomura, S. Kundu, T. Okada, Y. Sakata, S. Fukuzumi, *J. Phys. Chem. A* **2002**, *106*, 2803–2814; o) H. Imahori, K. Tamaki, Y. Araki, Y. Sekiguchi, O. Ito, Y. Sakata, S. Fukuzumi, *J. Am. Chem. Soc.* **2002**, *124*, 5165–5174; p) S. Fukuzumi, H. Imahori, *Mol. Supramol. Photochem.* **2003**, *9*, 227–273.

[22] W. B. Davis, W. A. Svec, M. A. Ratner, M. R. Wasielewski, *Nature* **1998**, *396*, 60–63.

[23] G. Pourtis, D. Beljonne, J. Cornil, M. A. Ratner, J. L. Brédas, *J. Am. Chem. Soc.* **2002**, *124*, 4436–4447.

[24] a) P. Bäuerle, *Electronic Materials: The Oligomer Approach* (Eds.: K. Müllen, G. Wegner), Wiley-VCH, Weinheim, **1998**, Chapter 2; b) D. Fichou, *Handbook of Oligo- and Polythiophenes*, Wiley-VCH, Weinheim, **1998**.
[25] T. Otsubo, Y. Aso, K. Takimiya, *J. Mater. Chem.* **2002**, *12*, 2565–2575.
[26] B. Jiang, S. Yang, S. Jones, Jr., *Chem. Mater.* **1997**, *9*, 2031–2034.
[27] A. Osuka, N. Tanabe, S. Kawabata, I. Yamazaki, Y. Nishimura, *J. Org. Chem.* **1995**, *60*, 7177–7185.
[28] a) R. Fong, D. I. Schuster, H. Mi, S. R. Wilson, A. U. Khan, *Proc. Electrochem. Soc.* **1998**, 262–267; b) K. Yamada, H. Imahori, Y. Nishimura, I. Yamakazi, Y. Sakata, *Chem. Lett.* **1999**, *9*, 895–896.
[29] K. Komatsu, Y. Murata, N. Takimoto, S. Mori, N. Sugita, T. Wan, *J. Org. Chem.* **1994**, *59*, 6101–6102.
[30] P. Timmerman, L. E. Witschel, F. Diederich, C. Boudon, J. P. Gisselbrecht, M. Gross, *Helv. Chim. Acta* **1996**, *79*, 6–20.
[31] P. Timmerman, H. Anderson, R. Faust, J. F. Nierengarten, T. Habicher, P. Seiler, F. Diederich, *Tetrahedron* **1996**, *52*, 4925–4947.
[32] M. M. Pereira, G. Muller, J. I. Ordinas, M. E. Azenha, L. G. Arnaut, *J. Chem. Soc. Perkin Trans. 2* **2002**, *9*, 1583–1588.
[33] D. M. Guldi, B. Nuber, P. J. Bracher, C. A. Alabi, S. MacMahon, J. W. Kukol, S. R. Wilson, D. I. Schuster, *J. Phys. Chem. A* **2003**, *107*, 3215–3221.
[34] a) L. Echegoyen, L. E. Echegoyen, *Acc. Chem. Res.* **1998**, *31*, 593–601; $E_{1/2}^{RED1}$ of C_{60} is taken as -0.98 V as reported earlier: M. Oçafrain, M. A. Herranz, L. Marx, C. Thilgen, F. Diederich, L. Echegoyen, *Chem. Eur. J.* **2003**, *9*, 4811–4819.
[35] A. J. Bard, L. R. Faulkner, *Electrochemical Methods: Fundamentals and Applications*, 2nd ed., Wiley, New York, **2001**.
[36] S. L. Murov, I. Carmichael, G. L. Hug, *Handbook of Photochemistry* (Eds.: S. Murov, I. Carmichael, G. L. Hug), Marcel Dekker, New York, **1993**.
[37] Time-resolved fluorescence decay measurements gave a value of 3.0 ± 0.1 ns for ZnTPP.
[38] C. Luo, D. M. Guldi, H. Imahori, Y. Sakata, *J. Am. Chem. Soc.* **2000**, *122*, 6535–6551.
[39] a) J. Rodriguez, C. Kirmaier, D. Holten, *J. Am. Chem. Soc.* **1989**, *111*, 6500–6506; b) K. Kalyanadundaram, *Photochemistry of Polypyridine and Porphyrin Complexes*, Academic Press, London, **1992**.
[40] D. M. Guldi, K. D. Asmus, *J. Phys. Chem. A* **1997**, *101*, 1472–1481.
[41] J.-P. Gisselbrecht, N. N. P. Moonen, C. Boudon, M. B. Nielsen, F. Diederich, M. Gross, *Eur. J. Org. Chem.* **2004**, *14*, 2959–2972.
[42] a) A. Osuka, N. Tanabe, S. Kawabata, I. Yamazaki, Y. Nishimura, *J. Org. Chem.* **1995**, *60*, 7177–7185; b) V. S.-Y. Lin, M. J. Therien, *Chem. Eur. J.* **1995**, *1*, 645–651; c) S. M. LeCours, S. G. DiMagno, M. J. Therien, *J. Am. Chem. Soc.* **1996**, *118*, 11854–11864; d) S. M. LeCours, C. M. Philips, J. C. de Paula, M. J. Therien, *J. Am. Chem. Soc.* **1997**, *119*, 12578–12589; e) D. P. Arnold, D. A. James, *J. Org. Chem.* **1997**, *62*, 3460–3469; f) D. P. Arnold, G. A. Heath, D. A. James, *New J. Chem.* **1998**, *22*, 1377–1387; g) R. Kumble, S. Palese, V. S.-Y. Lin, M. J. Therien, R. M. Hochstrasser, *J. Am. Chem. Soc.* **1998**, *120*, 11489–11498; h) T. E. O. Screen, I. M. Blake, L. H. Rees, W. Clegg, S. J. Borwick, H. L. Anderson, *J. Chem. Soc. Perkin Trans. 1* **2002**, *3*, 320–329; i) J. T. Fletcher, M. J. Therien, *Inorg. Chem.* **2002**, *41*, 331–341; j) F. Odobel, S. Suresh, E. Blart, Y. Nicolas, J.-P. Quintard, P. Janvier, J.-Y. Le Questel, B. Illien, D. Rondeau, P. Richomme, T. Haupl, S. Wallin, L. Hammarstrom, *Chem. Eur. J.* **2002**, *8*, 3027–3046; k) N. P. Redmore, I. V. Rubtsov, M. J. Therien, *J. Am. Chem. Soc.* **2003**, *125*, 8769–8778; l) I. V. Rubtsov, K. Susumu, G. I. Rubtsov, M. J. Therien, *J. Am. Chem. Soc.* **2003**, *125*, 2687–2696; m) E. Hindin, R. A. Forties, R. S. Loewe, A. Ambroise, C. Kirmaier, D. F. Bocian, J. S. Lindsey, D. Holten, R. S. Knox, *J. Phys. Chem. B* **2004**, *108*, 12821–12832; n) P. Thamyongkit, J. S. Lindsey, *J. Org. Chem.* **2004**, *69*, 5796–5799; o) E. Hindin, C. Kirmaier, J. R. Diers, K. Tomizaki, M. Taniguchi, J. S. Lindsey, D. F. Bocian, D. Holten, *J. Phys. Chem. B* **2004**, *108*, 8190–8200; p) P. Thamyongkit, M. Speckbacher, J. R. Diers, H. L. Kee, C. Kirmaier, D. Holten, D. F. Bocian, J. S. Lindsey, *J. Org. Chem.* **2004**, *69*, 3700–3710; q) K. Tomizaki, A. B. Lysenko, M. Taniguchi, J. S. Lindsey, *Tetrahedron* **2004**, *60*, 2011–2023; r) P. J. Angiolillo, H. T. Uyeda, T. V. Duncan, M. J. Therien, *J. Phys. Chem. B* **2004**, *108*, 11893–11903.
[43] a) K. Kils, J. Kajanus, J. Martensson, B. Albinsson, *J. Phys. Chem. B* **1999**, *103*, 7329–7339; b) J. Kajanus, S. B. Van Berlekom, B. Albinsson, J. Martensson, *Synthesis* **1999**, *7*, 1155–1162; c) J. Andreasson, J. Kajanus, J. Martensson, B. Albinsson, *J. Am. Chem. Soc.* **2000**, *122*, 9844–9845; d) K. Kils, J. Kajanus, A. N. Macpherson, J. Martensson, B. Albinsson, *J. Am. Chem. Soc.* **2001**, *123*, 3069–3080; e) A. Kyrychenko, B. Albinsson, *Chem. Phys. Lett.* **2002**, *366*, 291–299; f) J. Andreasson, G. Kodis, T. Ljungdahl, A. L. Moore, T. A. Moore, D. Gust, J. Martensson, B. Albinsson, *J. Phys. Chem. A* **2003**, *107*, 8825–8833; g) K. Pettersson, K. Kils, J. Martensson, B. Albinsson, *J. Am. Chem. Soc.* **2004**, *126*, 6710–6719.
[44] a) T. Drovetskaya, C. A. Reed, *Tetrahedron Lett.* **1995**, *36*, 7971–7974; b) M. G. Ranasinghe, A. M. Oliver, D. F. Rothenfluh, A. Salek, M. N. Padden-Row, *Tetrahedron Lett.* **1996**, *37*, 4797–4800; c) D. Kuciauskas, S. Lin, G. R. Seely, A. L. Moore, T. A. Moore, D. Gust, T. Drovetskaya, C. A. Reed, P. D. W. Boyd, *J. Phys. Chem.* **1996**, *100*, 15926–15932; d) T. D. M. Bell, K. P. Ghiggino, K. A. Jolliffe, M. G. Ranasinghe, S. J. Langford, M. J. Shephard, M. N. Paddon-Row, *J. Phys. Chem. A* **2002**, *106*, 10079–10088; e) T. J. Kesti, N. V. Tkachenko, V. Vehmanen, H. Yamada, H. Imahori, S. Fukuzumi, H. Lemmetyinen, *J. Am. Chem. Soc.* **2002**, *124*, 8067–8077; f) T. J. Kesti, N. V. Tkachenko, H. Yamada, H. Imahori, S. Fukuzumi, H. Lemmetyinen, *Photochem. Photobiol. Sci.* **2003**, *2*, 251–258.
[45] P. M. Burbank, J. R. Gibson, H. C. Dorn, M. R. Anderson, *J. Electroanal. Chem.* **1996**, *417*, 1–4.
[46] J. Crassous, J. A. Rivera, N. S. Fender, L. Shu, L. Echegoyen, C. Thilgen, A. Herrmann, F. Diederich, *Angew. Chem.* **1999**, *111*, 1716–1721; *Angew. Chem. Int. Ed.* **1999**, *38*, 1613–1617.

Received: December 28, 2004
Published online: March 31, 2005